

Missing data imputation using a truncated infinite factor model with application to metabolomics data

Kate Finucane¹, Lorraine Brennan², and Isobel Claire Gormley^{*1}

¹School of Mathematics and Statistics, University College Dublin.

²School of Agriculture and Food Science, University College Dublin, Ireland.

Abstract

In metabolomics, the study of small molecules in biological samples, data are often acquired through mass spectrometry. The resulting data contain highly correlated variables, typically with a larger number of variables than observations. Missing data are prevalent, and imputation is critical as data acquisition can be difficult and expensive, and many analysis methods necessitate complete data. In such data, missing at random (MAR) missingness occurs due to acquisition or processing error, while missing not at random (MNAR) missingness occurs when true values lie below the threshold for detection. Existing imputation methods generally assume one missingness type, or impute values outside the physical constraints of the data, which lack utility.

A truncated factor analysis model with an infinite number of factors (tIFA) is proposed to facilitate imputation in metabolomics data, in a statistically and physically principled manner. Truncated distributional assumptions underpin tIFA, ensuring cognisance of the data's physical constraints when imputing. Further, tIFA allows for both MAR and MNAR missingness, and a Bayesian inferential approach provides uncertainty quantification for imputed values and missingness types. The infinite

*claire.gormley@ucd.ie

factor model parsimoniously models the high-dimensional, multicollinear data, with nonparametric shrinkage priors obviating the need for model selection tools to infer the number of latent factors.

A simulation study is performed to assess the performance of tIFA and an application to a urinary metabolomics dataset results in a full dataset with practically useful imputed values, and associated uncertainty, ready for use in metabolomics analyses. Open-source R code accompanies tIFA, facilitating its widespread use.

1 Introduction

Metabolomics is the study of small molecules in biological samples, referred to as metabolites. The metabolome is the complement of metabolites in a sample, which can reveal information about altered metabolic pathways when examined under different conditions (Kosmidis et al., 2013; Zhong et al., 2022). Applications of metabolomics span from disease biomarker discovery (Tounta et al., 2021) to food and nutrition research (LeVatte et al., 2021), with the main data acquisition technologies being nuclear magnetic resonance spectroscopy (NMR) and mass spectrometry (MS) (Spicer et al., 2017).

Several characteristics of metabolomics data present challenges from a statistical modelling viewpoint. Metabolomics studies typically generate data in which the number of observations, n , is much smaller than the number of variables, p , which presents a challenge for many statistical modelling tools, such as regression-based methods, as they cannot operate in this regime (Worley and Powers, 2013; Zhao et al., 2019). Further, the variables in metabolomics data are often highly correlated with each other, again posing challenges for some statistical models (Blaise et al., 2016). Many tools exist to aid in the processing and analysis of such data (Wishart et al., 2022; Pang et al., 2024) and dimension reduction techniques are often utilised to address the issues of $n \ll p$ and multicollinearity (Wörheide et al., 2021). Factor analysis is one such technique used in metabolomics (Liland, 2011; Meng et al., 2016; Murphy et al., 2020) whereby variation in a dataset with many variables is described by a smaller number of underlying latent factors.

Although metabolomics data are comprehensive and high-dimensional, missing data

are a prevalent feature (Taylor et al., 2021; Sun and Xia, 2024). Two types of missingness are typical in metabolomics data: missing at random (MAR) data, which arise when a metabolite is present but is undetected due to technical or processing errors, and missing not at random (MNAR) data, which arise when either a metabolite is not present or it is present but at a concentration below the limit of detection (LOD) (Wilson et al., 2022).

Many methods exist for missing data imputation in general. Fixed-value imputation methods, such as variable-specific mean, median, half-minimum, or minimum-value imputation are common (Gromski et al., 2014; Wei et al., 2018b; Sun and Xia, 2024) but discouraged as they can distort the distribution of the data, introducing bias (Little and Rubin, 2020). More sophisticated approaches exist, such as k -nearest-neighbours-truncation (KNN-TN) (Shah et al., 2017), imputation using singular value decomposition (SVD) (Hastie and Mazumder, 2021), Gsimp (Wei et al., 2018a), Bayesian principal component analysis (BPCA) (Oba et al., 2003), and random forest (RF) models, e.g., Stekhoven and Bühlmann (2012). However, many such methods operate under the conservative assumption of the presence of only one missingness type. For example, Gsimp is designed for MNAR left-censored missingness only; MAR imputation is possible using Gsimp but only in the case where there is MAR missingness only. Additionally, due to the physical properties of metabolomics data non-negative imputed values are required, and while some imputation methods do impute within the domain of the observed data (e.g., KNN-TN), other methods exhibit no such restriction (e.g., SVD imputation). This can lead to negative values being imputed which are not useful for metabolomic analysis.

To ensure imputation of physically meaningful values and cognisance of different missing data types, while accounting for the multicollinearity and $n \ll p$ characteristics of metabolomic spectrometry data, a truncated factor analysis model with an infinite number of factors (tIFA) is proposed. Inspired by the BayesMetab framework (Shah et al., 2019), tIFA imputes missing data under the assumption of a truncated multivariate normal factor analysis model, thereby respecting the physical constraints of the data and inducing parsimony given the $n \ll p$ setting. Similar to BayesMetab, tIFA maintains the ability to impute MAR and MNAR data appropriately and simultaneously. In contrast to impu-

tation methods which do not have a probabilistic basis, tIFA’s underpinning probabilistic model and inference in the Bayesian framework naturally allow uncertainty quantification of the imputed values, and the missingness type. Thus, tIFA allows for missing data to be imputed in a statistically and physically principled manner, with the inherent uncertainties in the imputed values available.

In what follows, Section 2 introduces a urinary metabolomics dataset which motivates and illustrates the tIFA model. Interest lies in imputing the missing data in a manner which is cognisant of both the MAR and MNAR missingness types that are likely to be present, while respecting the data’s multicollinearity and physically-enforced non-negative support, and while quantifying the uncertainty associated with each imputed value. Section 3 outlines tIFA and its imputation approach and provides details on inference. Section 4 details a simulation study performed to assess the performance of tIFA and in Section 5 tIFA is used to impute missing values in the urinary metabolomics dataset. Section 6 concludes with a discussion. To facilitate widespread use of tIFA, associated R code is available at github.com/kfinucane/tIFA, with which all results herein were produced.

2 A urinary metabolomics dataset

A urinary metabolomics dataset motivates and illustrates the proposed tIFA approach. The dataset is a liquid chromatography mass spectrometry (LC-MS) dataset resulting from a study that measured the postprandial response to consumption of food, in this case broccoli (McNamara et al., 2023). The study included 18 participants, pre and post-consumption of cooked broccoli. The LC-MS data used in the current work are from the baseline pre-consumption samples. The dataset included $n = 18$ participants and 2032 variables. Ethical approval was granted by the UCD Sciences Human Research Ethics Committee (LS-15-69-Brennan). All participants provided written informed consent.

As removing variables with $> 20\%$ missingness is typical in metabolomics research (Bijlsma et al., 2006), here a total of 68 variables, that had a conservatively higher $> 25\%$ of their entries missing, were removed prior to analysis. The missingness level in the final dataset, where $n = 18$ and $p = 1964$, is 2.69%. Figure 1 illustrates the final dataset, and

the missingness proportion across all retained variables.

3 Imputation via a Bayesian truncated infinite factor model

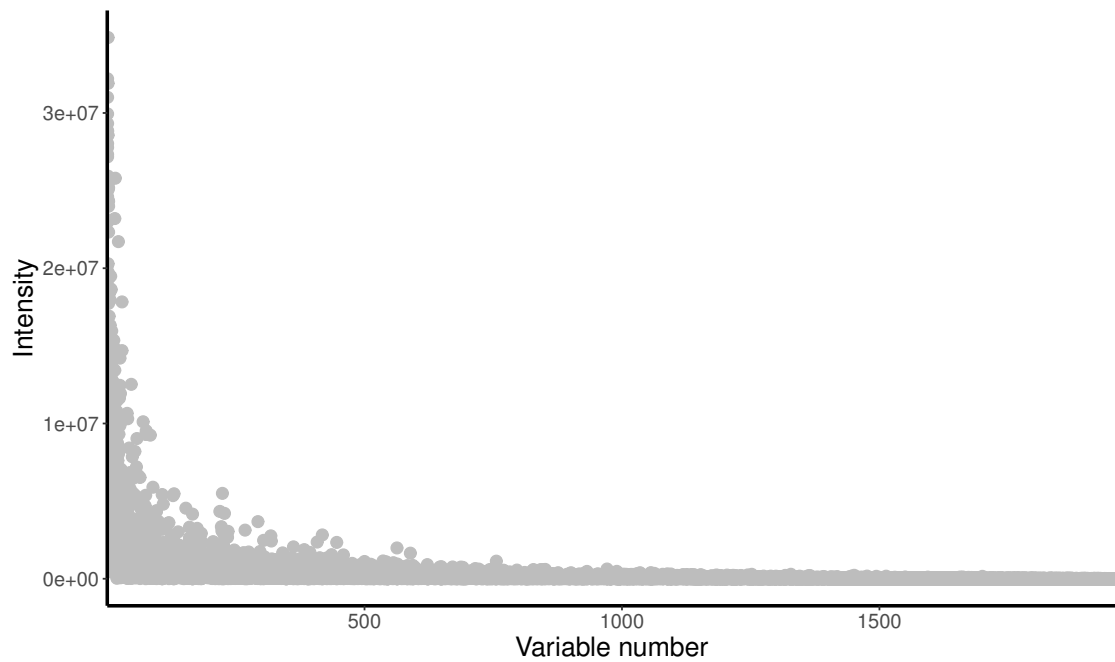
Due to their parsimony, factor analytic models are popular approaches for modelling high-dimensional, multicollinear data where $n \ll p$. Factor analytic models model the observed data as a linear combination of latent factors where their number, k , is much lower than p (Bartholomew et al., 2011). In the context of metabolomics data, factor analytic models have been used, for example, in dynamic modelling of the metabolome (Nordin et al., 2024), molecule classification (Huang et al., 2018), and biomarker identification (D’Angelo et al., 2021). Inspired by Shah et al. (2019), here an infinite factor analysis model (Bhattacharya and Dunson, 2011) is employed to model metabolomics data with the aim of imputing missing values in a statistically and physically principled manner; to achieve this, a truncated factor analysis model is employed, congruent with the physical properties of the data.

3.1 The tIFA model

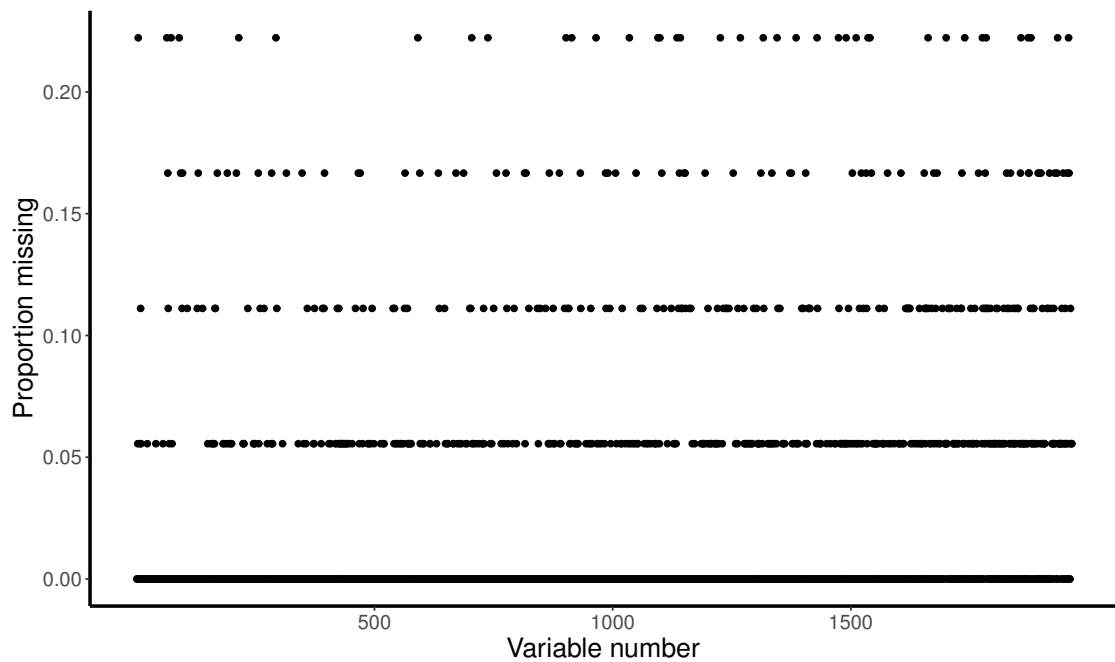
The general form of a factor model is

$$\mathbf{y}_i = \boldsymbol{\mu} + \mathbf{\Lambda}\boldsymbol{\eta}_i + \boldsymbol{\epsilon}_i, \quad i = 1, \dots, n \quad (1)$$

where $\mathbf{y}_i = (y_{i1}, \dots, y_{ip})^\top$ is the p -dimensional data vector of observation i in the $n \times p$ dataset \mathbf{Y} , $\boldsymbol{\mu}$ is a p -dimensional mean vector, $\mathbf{\Lambda}$ is a $p \times k$ loadings matrix, $\boldsymbol{\eta}_i$ is a k -dimensional latent factor score for observation i , typically assumed to be $N_k(\mathbf{0}, \mathbf{I}_k)$, and $\boldsymbol{\epsilon}_i$ is the specific error, assumed to be $N_p(\mathbf{0}, \boldsymbol{\Sigma})$ where $\boldsymbol{\Sigma} = \text{diag}(\sigma_1^2, \dots, \sigma_p^2)$. Under this model, given the latent factor $\boldsymbol{\eta}_i$, the observed variables y_{ij} , $j = 1, \dots, p$, are conditionally independent. Often, k is assumed to be finite and inferred from the data using, for example, an information criterion (e.g., McNicholas and Murphy (2008)). Infinite factor models assume k to be infinite and employ shrinkage priors on the loadings matrix (Bhattacharya and Dunson, 2011), obviating the need to fit and choose between multiple models with



(a)



(b)

Figure 1: (a) The untargeted urinary metabolomics data considered herein. (b) The proportion of missingness in each variable.

different values of k . Such models have received much attention in the literature, with recent work on e.g., generalised infinite factor models (Schiavon et al., 2022), novel shrinkage techniques (Legramanti et al., 2020; Frühwirth-Schnatter, 2023) and their use in the context of clustering (Murphy et al., 2020).

The BayesMetab method (Shah et al., 2019) for imputing missing values in metabolomics data employs an infinite factor analysis (IFA) model but makes the assumption that the observed data are Gaussian distributed. Such an assumption does not hold in the case of metabolomics data as these measurement data naturally do not contain negative values. Importantly, imputing missing values under such an assumption can lead to imputed values that are negative and not useful to a metabolomics user. Therefore, the tIFA approach aims to account for the physical constraints of the data, thereby facilitating imputation of physically feasible values. This is achieved by assuming the latent factor scores and the specific errors are constrained to lie on the positive real line, similar to D’Angelo et al. (2021), i.e., $\boldsymbol{\eta}_i \sim N_k^{[0,\infty)}(\mathbf{0}, \mathbf{I}_k)$ and $\boldsymbol{\epsilon}_i \sim N_p^{[0,\infty)}(\mathbf{0}, \boldsymbol{\Sigma})$ for $i = 1, \dots, n$ where, under the infinite factor model $k = \infty$. Given these assumptions and (1), under the tIFA model then conditionally

$$\mathbf{y}_i \mid \boldsymbol{\eta}_i \sim N_p^{[0,\infty)}(\boldsymbol{\mu} + \boldsymbol{\Lambda}\boldsymbol{\eta}_i, \boldsymbol{\Sigma}) \quad (2)$$

and, marginally, $\mathbf{y}_i \sim N_p^{[0,\infty)}(\boldsymbol{\mu}, \boldsymbol{\Lambda}\boldsymbol{\Lambda}^\top + \boldsymbol{\Sigma})$ for $i = 1, \dots, n$.

3.2 Accounting for missing data

As in BayesMetab, the tIFA approach facilitates imputation of both MAR and MNAR values in a statistically principled manner. A missingness indicator variable R_{ij} is introduced for observation i and variable j ; when y_{ij} is observed, $R_{ij} = 1$. However, when y_{ij} is missing, then $R_{ij} = 0$ and it is assumed that

$$\Pr(R_{ij} = 0 \mid y_{ij}) = \begin{cases} \alpha, & y_{ij} > \text{LOD} \\ 1, & y_{ij} \leq \text{LOD}. \end{cases}$$

This assumption allows for both types of missingness to occur: even if a true value is above the LOD, it can still be missing e.g., for technical reasons. Such a missing data type is

considered MAR, and here is assumed to happen with common probability α . Intuitively, if the true value of y_{ij} is lower than the LOD then y_{ij} will be missing and $R_{ij} = 0$ with probability 1; here the missing data type is MNAR. Such assumptions, combined with tIFA, allow for statistically and physically principled imputation of missing data in high-dimensional metabolomics data.

3.3 Prior distributions

Inference proceeds in a Bayesian framework, naturally facilitating quantification of the inherent uncertainty in the model parameters, imputed values and the associated missingness types. To complete the specification of the Bayesian tIFA model, an uninformative uniform prior is placed on α and the following prior distributions are assumed:

$$\begin{aligned}\boldsymbol{\mu} &\sim N_p^{[0,\infty)}(\tilde{\boldsymbol{\mu}}, \varphi^{-1}\mathbf{I}_p) \\ \lambda_{jh} &\sim N_1^{[0,\infty)}(0, \phi_{jh}^{-1}\tau_h^{-1}) \quad \text{for } j = 1, \dots, p \text{ and } h = 1, \dots, \infty \\ \sigma_j^{-2} &\sim \text{Ga}(a_\sigma, b_\sigma) \quad \text{for } j = 1, \dots, p\end{aligned}$$

A shrinkage prior is assumed for the variance of the prior on the loading λ_{jh} , which results in shrinkage of the factor loadings towards zero as the factor dimension h increases, inducing automatic inference on the number of effective factors required. This is achieved by assuming priors for the hyperparameters ϕ_{jh} , a local shrinkage parameter for variable j and factor h of the loadings matrix, and τ_h , a factor or column-wise global shrinkage parameter, as follows:

$$\begin{aligned}\phi_{jh} &\sim \text{Ga}(\kappa_1, \kappa_2), \quad \tau_h = \prod_{l=1}^h \delta_l \\ \delta_1 &\sim \text{Ga}(a_1, 1), \quad \delta_l \sim \text{Ga}^{[1,\infty)}(a_2, 1) \quad l = 2, \dots, \infty\end{aligned}$$

Here, as in [Gwee et al. \(2024\)](#), this multiplicative truncated gamma process (MTGP) shrinkage prior assumes a gamma prior, truncated to have support above 1, for δ_l for $l = 2, \dots, \infty$ in order to elicit the desired shrinkage behaviour. Similarly, care must be taken when specifying a_1 and a_2 to elicit the desired shrinkage behaviour across the columns of $\mathbf{\Lambda}$;

see [Durante \(2017\)](#) for a thorough discussion. Employing such a shrinkage prior eliminates the need to fit multiple tIFA models with different, finite values of k and then choose the optimal model among them using an often subjectively selected model selection criterion.

3.4 Inference and imputation

A Bayesian approach to inference and imputation under the tIFA model proceeds by employing a Markov chain Monte Carlo (MCMC) sampler to explore the joint posterior distribution. Given the likelihood function and prior distributions, the posterior distribution is

$$p(\boldsymbol{\mu}, \boldsymbol{\Lambda}, \boldsymbol{\eta}, \boldsymbol{\Sigma}, \boldsymbol{\phi}, \boldsymbol{\delta}, \alpha \mid \mathbf{Y}) \propto p(\mathbf{Y} \mid \boldsymbol{\mu}, \boldsymbol{\eta}, \boldsymbol{\Lambda}, \boldsymbol{\Sigma}) p(\boldsymbol{\mu}) p(\boldsymbol{\eta}) p(\boldsymbol{\Sigma}) p(\boldsymbol{\Lambda} \mid \boldsymbol{\phi}, \boldsymbol{\delta}) \\ p(\boldsymbol{\phi}) p(\boldsymbol{\delta}) p(\alpha).$$

where $\boldsymbol{\eta} = \{\boldsymbol{\eta}_1, \dots, \boldsymbol{\eta}_n\}$, $\boldsymbol{\phi} = \{\boldsymbol{\phi}_1, \dots, \boldsymbol{\phi}_p\}$ with $\boldsymbol{\phi}_j = (\phi_{j1}, \dots, \phi_{jk})^\top$ for $j = 1, \dots, p$, and $\boldsymbol{\delta} = (\delta_1, \dots, \delta_k)^\top$. The resulting full conditional posterior distributions of all parameters are available in closed form: the mean, loadings and latent factor scores have truncated Gaussian full conditional distributions while all other parameters have (truncated) gamma full conditional distributions, with the exception of the probability parameter α which has a beta full conditional distribution. As such, Gibbs sampling can be used to straightforwardly explore the posterior. The specification of the full conditional distributions, and their derivations, are provided in [A](#) and [B](#) respectively. Of note is the practical treatment of the number of factors when running the MCMC chain: while k is assumed to be infinite, for computation k is approximated by a finite value k^* .

Missing data entries are imputed during the MCMC procedure. When y_{ij} is missing (i.e., $R_{ij} = 0$), a missingness designation indicator variable Z_{ij} is introduced such that $Z_{ij} = 0$ when y_{ij} is MAR, and $Z_{ij} = 1$ when y_{ij} is MNAR. At each iteration of the MCMC chain, conditional on all other parameter values, Z_{ij} is sampled by drawing from a Bernoulli trial with success probability $\Pr(Z_{ij} = 1 \mid R_{ij} = 0) = P/(P + \alpha Q)$ where

$$P = \int_0^{\text{LOD}} N_1^{[0, \infty)}(\dot{\mu}_{ij}, \dot{\sigma}_j^2) dy_{ij} \quad \text{and} \quad Q = \int_{\text{LOD}}^{\infty} N_1^{[0, \infty)}(\dot{\mu}_{ij}, \dot{\sigma}_j^2) dy_{ij}.$$

where, $\dot{\mu}_{ij}$ denotes the ij^{th} element of the current value of $\boldsymbol{\mu} + \boldsymbol{\Lambda}\boldsymbol{\eta}_i$ and $\dot{\sigma}_j^2$ denotes the current value of the j^{th} diagonal element of $\boldsymbol{\Sigma}$. Imputation is then performed by drawing a sample from the relevant truncated Gaussian distribution, given the missingness designation variable: if $Z_{ij} = 1$ then $y_{ij} \mid Z_{ij} \sim N_1^{(0, \text{LOD})}(\dot{\mu}_{ij}, \dot{\sigma}_j^2)$ and if $Z_{ij} = 0$ then $y_{ij} \mid Z_{ij} \sim N_1^{(\text{LOD}, \infty)}(\dot{\mu}_{ij}, \dot{\sigma}_j^2)$.

Each iteration of the MCMC chain provides a complete dataset with entries imputed independently, conditional on all other current parameters. On convergence of the MCMC chain, here the posterior mean of the imputed values for each missing entry is used as its imputed value. Other relevant summaries of the sampled imputed values over the MCMC chain can be easily obtained and used, for example, for the construction of credible intervals providing uncertainty quantification and deeper, more insightful inference for the user.

4 Simulation study

A simulation study was conducted to assess the imputation performance of the tIFA approach and to compare its performance to state-of-the-art imputation methods.

4.1 Simulation study set up

Simulated data that emulate the characteristics of the urinary metabolomics dataset (see Section 2) were considered. Ten datasets, each with $n = 18$ and $p = 1300$, were simulated from the tIFA model in (2) with $k^* = 2$. For each dataset, the mean $\boldsymbol{\mu}$ was simulated from the prior specified in Section 3.3 with $\tilde{\boldsymbol{\mu}}$ the sample mean of p randomly selected (without replacement) fully-observed variables from the urinary metabolomics dataset and $\varphi = 2$, ensuring little difference between $\boldsymbol{\mu}$ and the urinary metabolomics data sample mean. Principal component analysis (PCA) was applied to the selected fully-observed variables and $\boldsymbol{\Lambda}$ was fixed as the absolute value of the resulting loadings matrix. For observation i , $\boldsymbol{\eta}_i \sim N_{k^*}^{(0, \infty)}(\mathbf{0}, \mathbf{I}_{k^*})$ and $\boldsymbol{\epsilon}_i \sim N_p(\mathbf{0}, \boldsymbol{\Sigma})$, where $\text{diag}(\boldsymbol{\Sigma})$ was set to the diagonal of the covariance matrix of $\tilde{\boldsymbol{\mathcal{E}}} = (\tilde{\boldsymbol{\epsilon}}_1, \dots, \tilde{\boldsymbol{\epsilon}}_n)^\top$ where $\tilde{\boldsymbol{\epsilon}}_i = \tilde{\boldsymbol{y}}_i - \boldsymbol{\mu} - \boldsymbol{\Lambda}\boldsymbol{\eta}_i$ where $\tilde{\boldsymbol{y}}_i$ are the p selected fully-observed variables from observation i .

Missingness under the two missing data types was then introduced to emulate the total missingness proportion in the urinary metabolomics dataset. Similar to the approach in [Wei et al. \(2018b\)](#), for each simulated dataset the variables were sorted by lowest minimum value in ascending order, and the lowest-ranked $\text{Ceil}(0.07p)$ identified. The n entries of each of these lowest-ranked variables were then sorted in ascending order; the smallest $\text{Ceil}(\text{Unif}(0.1, 0.2)n)$ entries for each variable were designated MNAR, and removed. Additionally, all entries < 3000 were removed and designated MNAR. For MAR missingness, in each simulated dataset, 1.5% of the remaining non-missing entries were randomly selected and removed. The resulting datasets contained, on average, 1.5% MAR and 2.7% MNAR entries, with a total missingness proportion of 4.2%.

The tIFA model was fitted to each simulated dataset using R ([R Core Team, 2024](#)), running MCMC chains for 10000 iterations, with a 5000 burn-in and every fifth thinned. Imputed values were initialised as the absolute values of SVD imputed values using the `softImpute` R package ([Hastie and Mazumder, 2021](#)). Hyperparameters were set following [Shah et al. \(2019\)](#) and [Murphy et al. \(2020\)](#): $\tilde{\boldsymbol{\mu}}$ was set to the sample mean with $\varphi = 0.1$, $\kappa_1 = 3$, $\kappa_2 = 2$, $a_\sigma = 1$, $b_\sigma = 0.3$, and, for the MTGP, $a_1 = 2.1$, $a_2 = 3.1$, as in [Durante \(2017\)](#) and [Gwee et al. \(2024\)](#). Initial values of $\boldsymbol{\Lambda}$ were the absolute value of the data’s PCA loadings and $\boldsymbol{\Sigma}$ was initialised using the same approach as in the data simulation. Finally, the number of latent factors was $k^* = 5$ during model fitting. While use of an adaptive Gibbs sampler ([Bhattacharya and Dunson, 2011](#)), which facilitates the addition and removal of factors as the MCMC evolves, was explored, little inferential benefit and greater computational cost was observed. Further, fixing $k^* > 5$ resulted in factor splitting where the data’s common variation spread over too many factors, while using too few was insufficient to describe the variation in the data.

For comparative purposes, missing values were also imputed using fixed-value imputation methods (zero, half-minimum, and mean imputation), SVD imputation, RF imputation using the `missForest` R package ([Stekhoven, 2022](#)), and IFA imputation ([Shah et al., 2019](#)). To assess performance, for each simulated dataset the mean absolute error (MAE) and residuals between posterior mean imputed values and true values were computed for

all methods considered. Where available, credible intervals are also reported.

4.2 Simulation study results

Figure 2a illustrates imputation performance overall, for both MAR and MNAR missingness. Of the fixed-value imputation methods, the zero and half-minimum approaches exhibit poorer performance than mean imputation, with larger and more variable MAEs. While the RF method performs similarly to mean imputation, the SVD and IFA approaches perform poorly, with MAEs larger and more variable than RF imputation. The tIFA method performs similarly to mean and RF imputation, with similar MAE values and variability. A similar performance pattern is observed when imputation of MAR entries only is considered (Figure 2b), where the MAR designation refers to the true missing data type.

Imputation performance on the MNAR entries, where the MNAR designation refers to the true missing data type, exhibits a different trend (Figure 2c). The zero and half-minimum imputation methods perform well, as these methods impute fixed-values which, due to the LOD in LC-MS data, will not be far from the truth. The mean, SVD, and RF methods exhibit similar results, with higher MAEs than the fixed-value methods. The IFA method appears to perform well, however, the low MAEs come at a cost as physically impossible negative values are imputed. The same is true of SVD imputation, without the performance boost. The tIFA method shows similar MNAR imputation performance to the mean and RF methods, with the lowest median MAE.

Details of the residuals between the posterior mean imputed values and true values across all simulated datasets are available in C, along with residuals for a single simulated dataset for each imputation method. Performance trends in the residuals are similar to those exhibited by the MAE.

Figure 3 illustrates the true versus imputed values for a single simulated dataset, using the mean, IFA and tIFA approaches (similar figures for the other imputation methods considered are in C). Under mean imputation (Figure 3a), only a point estimate is imputed for each missing value and no measure of uncertainty is readily available; if there are multiple missing entries in one variable the same fixed value is imputed for all of them.

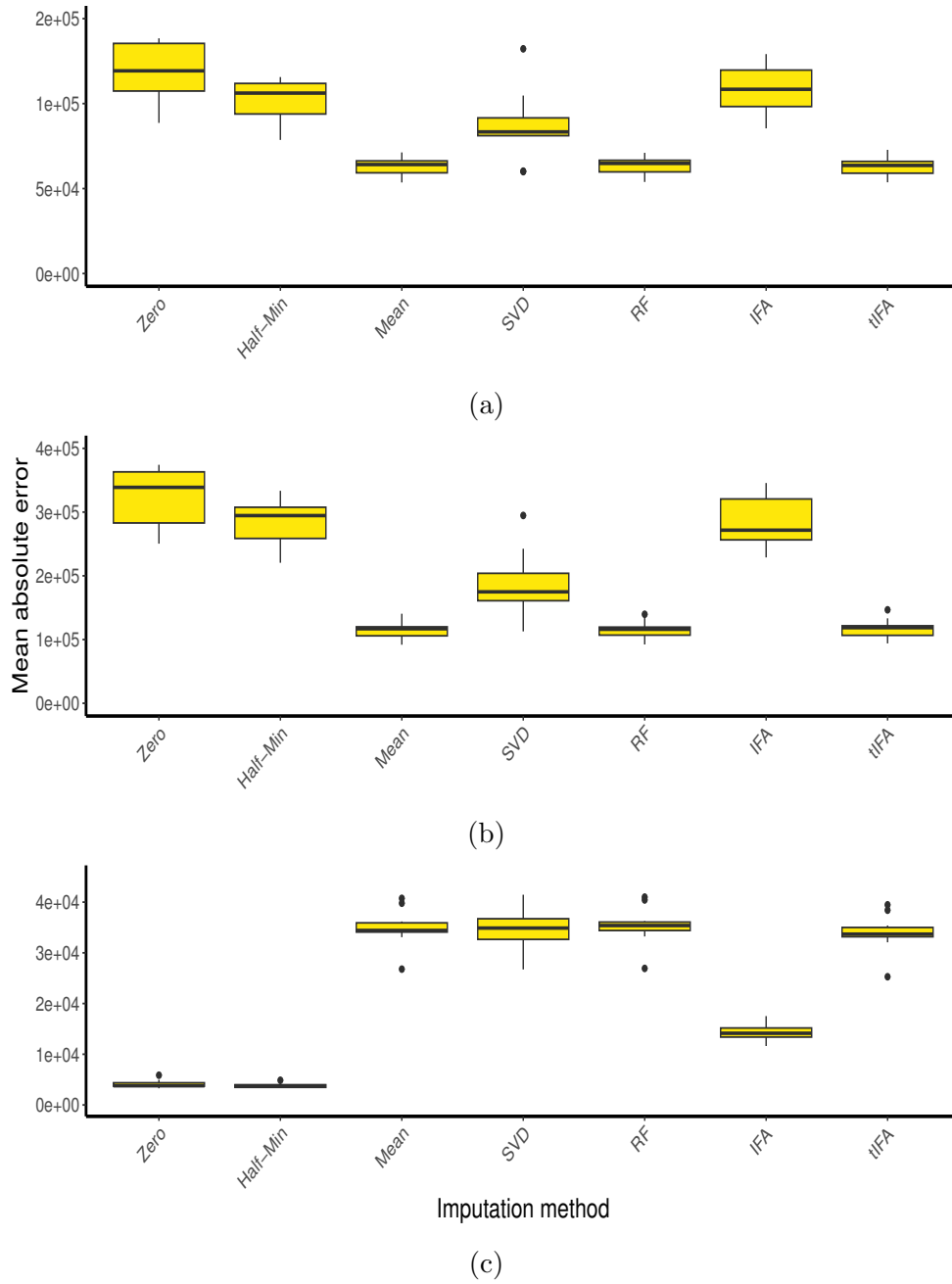


Figure 2: Mean absolute errors between posterior mean imputed values and true values across ten simulated datasets for (a) all imputed values, (b) MAR imputed values and (c) MNAR imputed values, across all imputation methods.

Additionally, imputation below the assumed LOD is not possible under mean imputation meaning that the truly MNAR entries are not appropriately imputed. In Figure 3b, the IFA approach imputes missing data with impractical negative values, but does quantify the uncertainty associated with the imputed values. Under tIFA, Figure 3c illustrates physically meaningful posterior mean imputed values and their associated 95% credible intervals; these summaries are readily available and provide richer inference for the user. Under tIFA for this simulated data set, the designation accuracy for truly MAR entries was 90% while for truly MNAR entries, designation accuracy was 40%. However, truly MNAR entries are imputed sensibly, even when designated as MAR, with values above the LOD but in the range of their respective variable’s observed data. Intuitively, across all methods, imputed values for truly lower-valued missing entries tend to be overestimated, as these are likely MNAR entries whose imputed values will be biased upwards as data are not observed below the LOD.

5 Imputing missing values in the urinary metabolomics data

The tIFA approach, with $k^* = 5$, was used to impute missing data in the urinary metabolomics dataset detailed in Section 2. For comparative purposes, imputation via existing methods (zero, half-minimum, mean, SVD, RF and IFA imputation) were also considered.

Figure 4 provides violin plots of two observed variables that have relatively large values and variances; for such variables it is likely that any missing values would be MAR as the observed values are far from the LOD. Variable 41 (Figure 4a) has only one missing entry while variable 64 (Figure 4b) has four. Figure 4 also illustrates the imputed values, and associated uncertainty where available. For both variables, the fixed-value imputation methods (zero, half-minimum, and mean imputation) do not provide uncertainty quantification, and in the case of variable 64 impute the same value for each missing entry. The SVD and IFA approaches impute reasonable values in the case of variable 41, however, in variable 64 inappropriate negative values are imputed; the IFA method does, however,

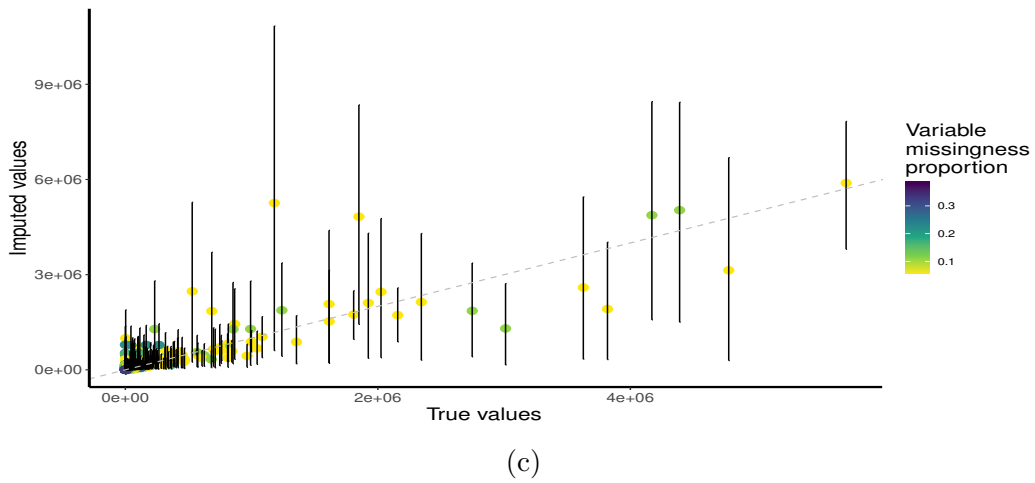
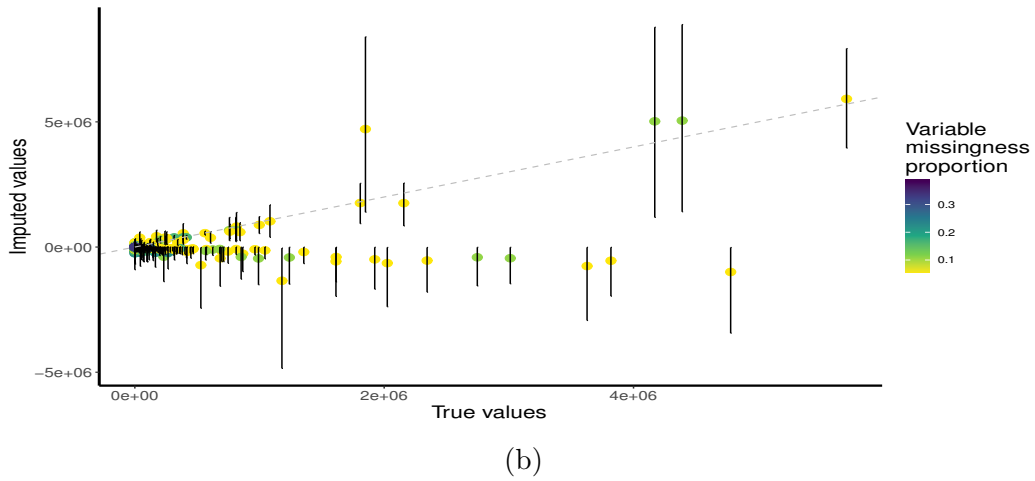
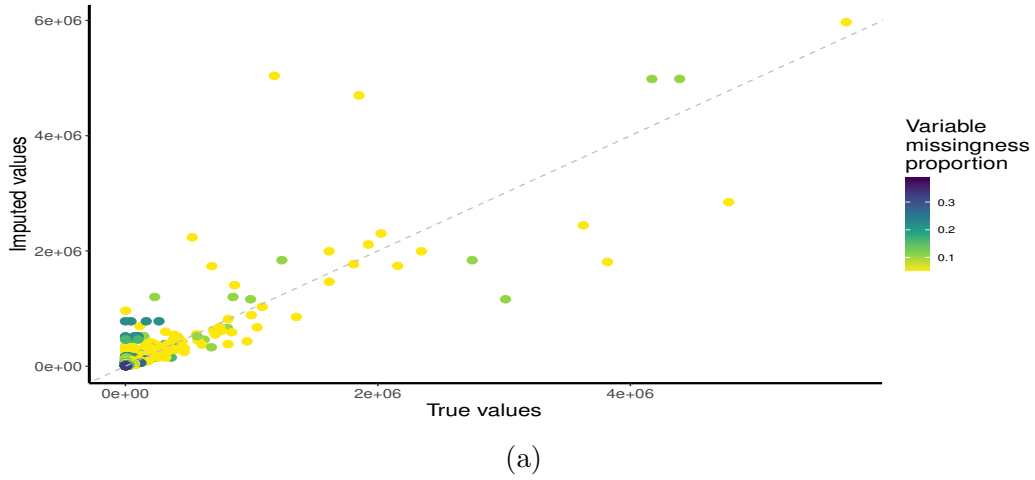
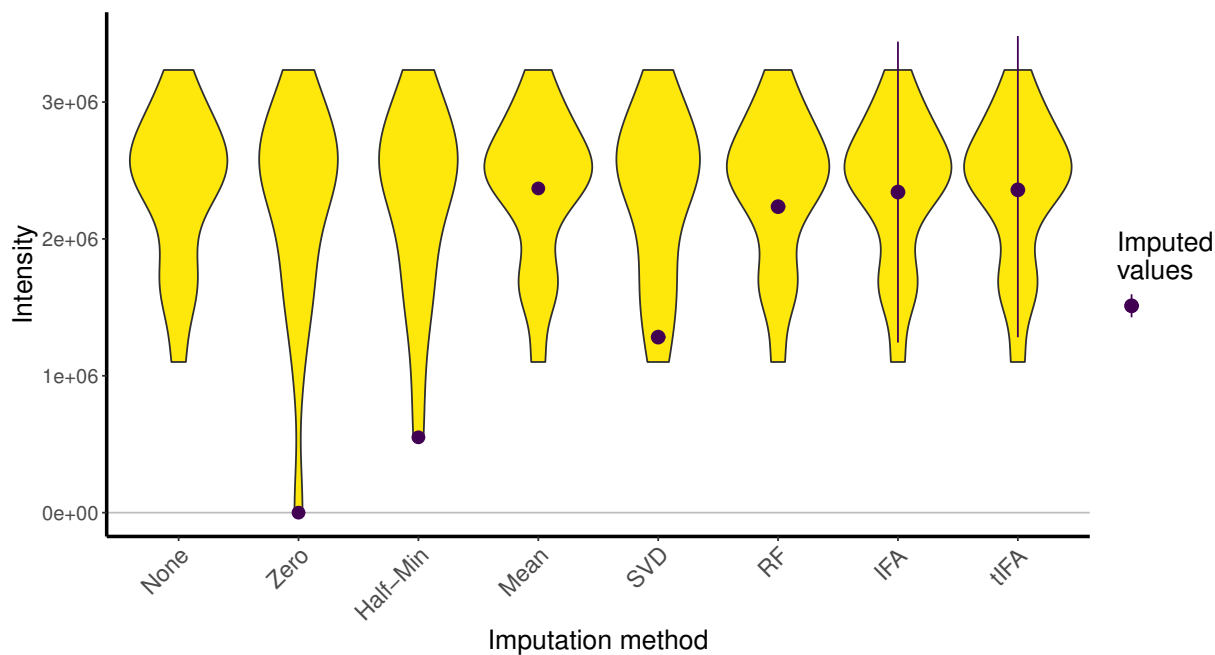


Figure 3: For one simulated data set, true values versus (a) imputed values under mean imputation (b) posterior mean imputed values, and associated 95% credible intervals, under IFA imputation and (c) posterior mean imputed values, with associated 95% credible intervals, under tIFA imputation. The dashed grey line is the line of equality and points are coloured by their variable's proportion of missingness.

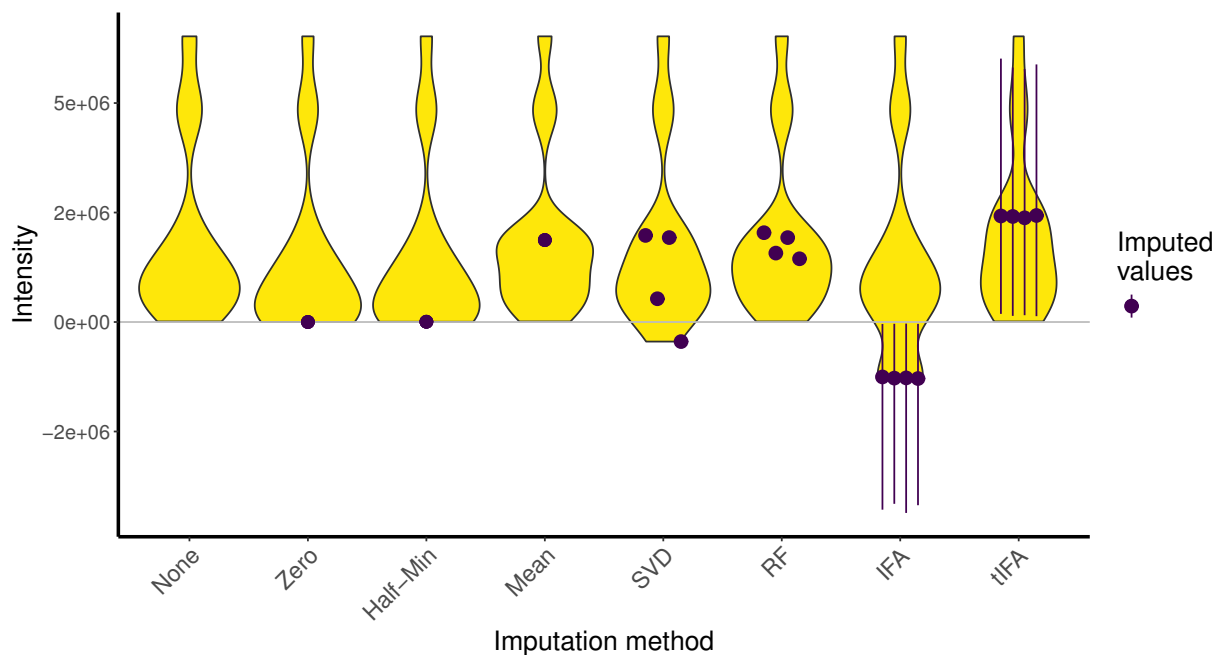
provide uncertainty quantification. For the RF approach, plausible values are imputed, but no uncertainty is provided. In contrast, the tIFA model provides physically plausible posterior mean imputed values, and 95% credible intervals for both variables.

Figure 5 provides violin plots and imputed values for another two variables, variable 1874 (Figure 5a) and variable 1917 (Figure 5b). Both have three missing values and have relatively low means and variances; MNAR missingness is likely to be present here. The fixed-value imputation methods again have limited utility, while the SVD and IFA approaches impute non-meaningful negative values. The RF method imputes plausible values, however, is restricted to the observed domain of the data and therefore does not handle MNAR missingness. The tIFA model imputes quite different values for the two variables: in variable 1874, the three missing entries are designated as MAR (with posterior probabilities 0.550, 0.581, and 0.565, respectively) and imputed accordingly. For variable 1917, the missing entries are designated as MNAR (with posterior probabilities 0.737, 0.773 and 0.763 respectively). The true values of these entries are of course unknown, however, the imputed values demonstrate the flexibility of the tIFA approach to allow for MAR and MNAR missingness, and provide physically meaningful associated credible intervals.

Finally, Figure 6 shows imputed and observed values for the variables with missingness. All variables with missing entries are presented in Figure 6a while Figure 6b only shows the variables with lowest observed means to provide a clearer view of their mixed imputation types and varying designation uncertainties. In general, for variables with larger observed means and variances the tIFA method designates missing values as MAR and imputes plausible values within the range of the observed values; this is intuitive as the observed values are not close to the LOD. In variables with lower observed means and variances (Figure 6b), the tIFA model infers a mix of both MAR and MNAR-designated imputations. On average, the tIFA model imputes MAR-designated entries with lower designation-uncertainty than MNAR values (0.194 versus 0.371, respectively). However, the variability in designation-uncertainty is higher in MAR-designated entries compared to MNAR-designated entries (standard deviations of 0.148 versus 0.083, respectively). In summary, imputation using the tIFA approach allows for both types of missingness, results

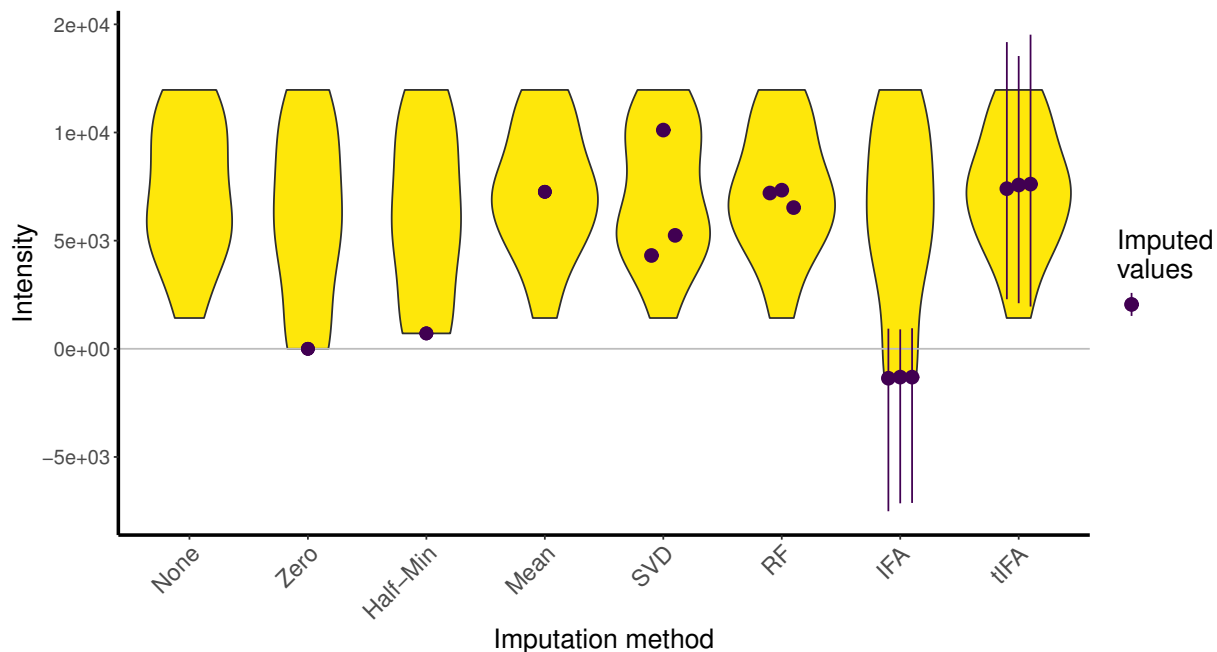


(a)

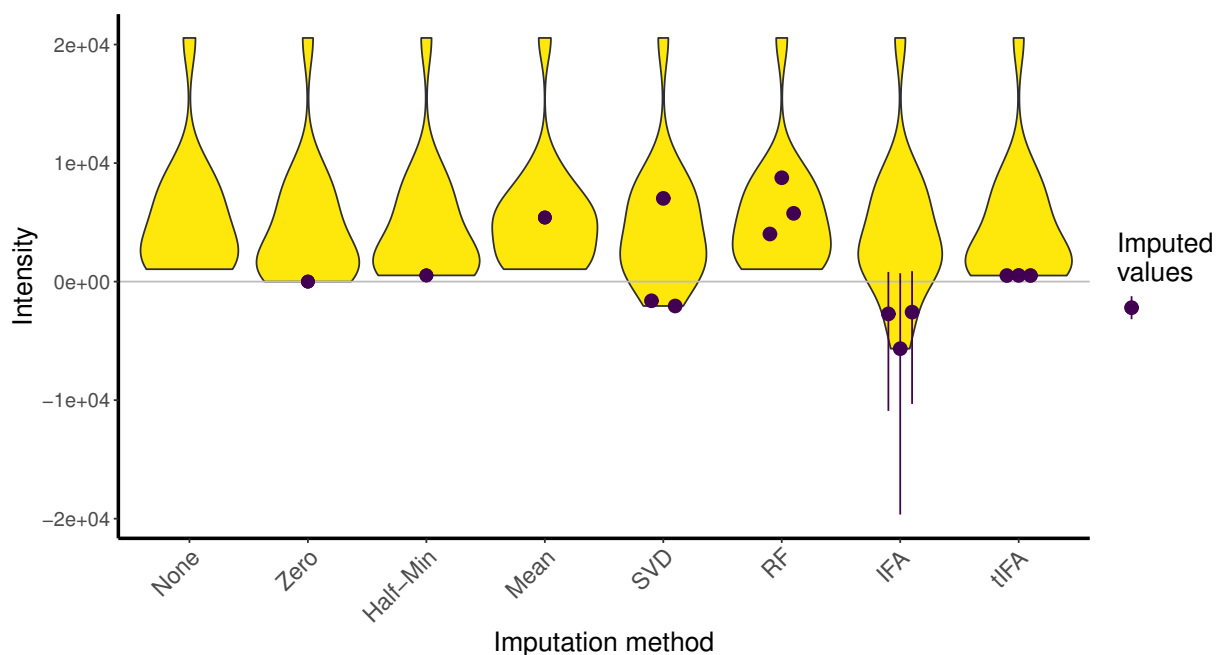


(b)

Figure 4: Violin plots and imputed values for two variables with high mean values and variances from the urinary metabolomics dataset: (a) variable 41 which has one missing value and (b) variable 64 which has four missing values. For mean, half-minimum and zero imputation, only one imputed point is visible, as all missing entries are imputed with the same value. For imputation methods that impute different values for different missing values, imputed values are jittered for clarity. Where available, 95% credible intervals are provided.



(a)



(b)

Figure 5: Violin plots and imputed values for two variables with low means and variances from the urinary metabolomics dataset: (a) variable 1874 and (b) variable 1917, both of which have three missing values. For zero, half-minimum, and mean imputation, only one imputed point is visible, as all missing entries are imputed with the same value. Imputation methods which impute different values for missing entries in the same variable are jittered for clarity, and 95% credible intervals are shown where available.

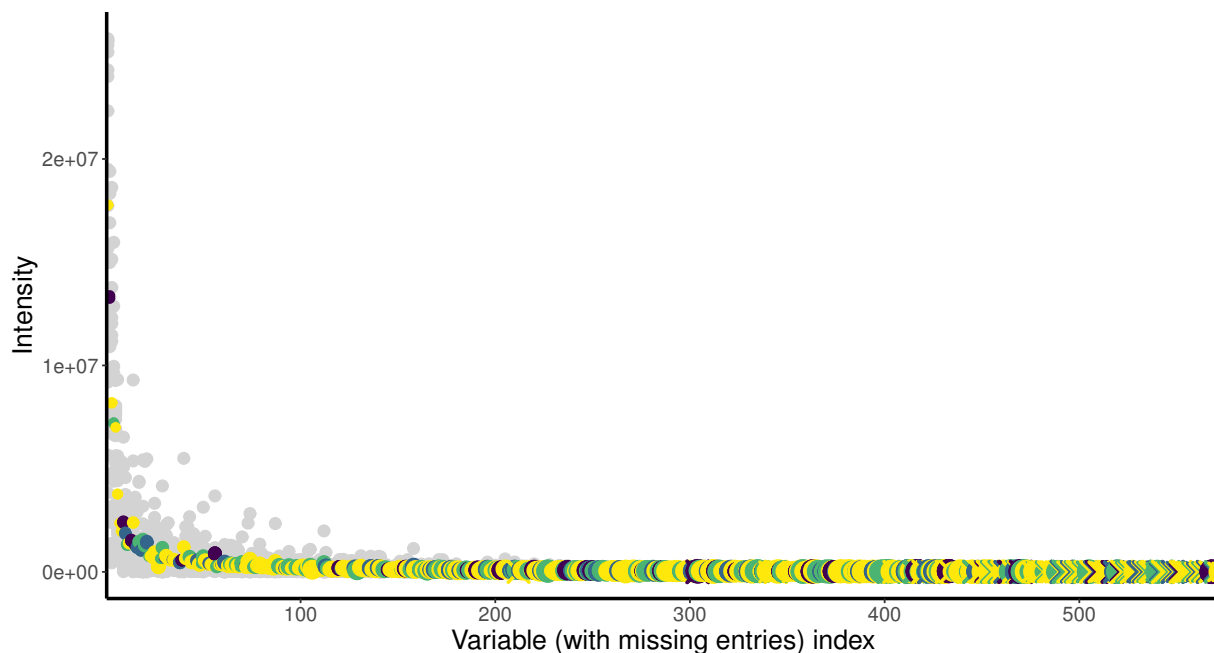
in physically plausible values, and provides uncertainty quantification.

6 Discussion

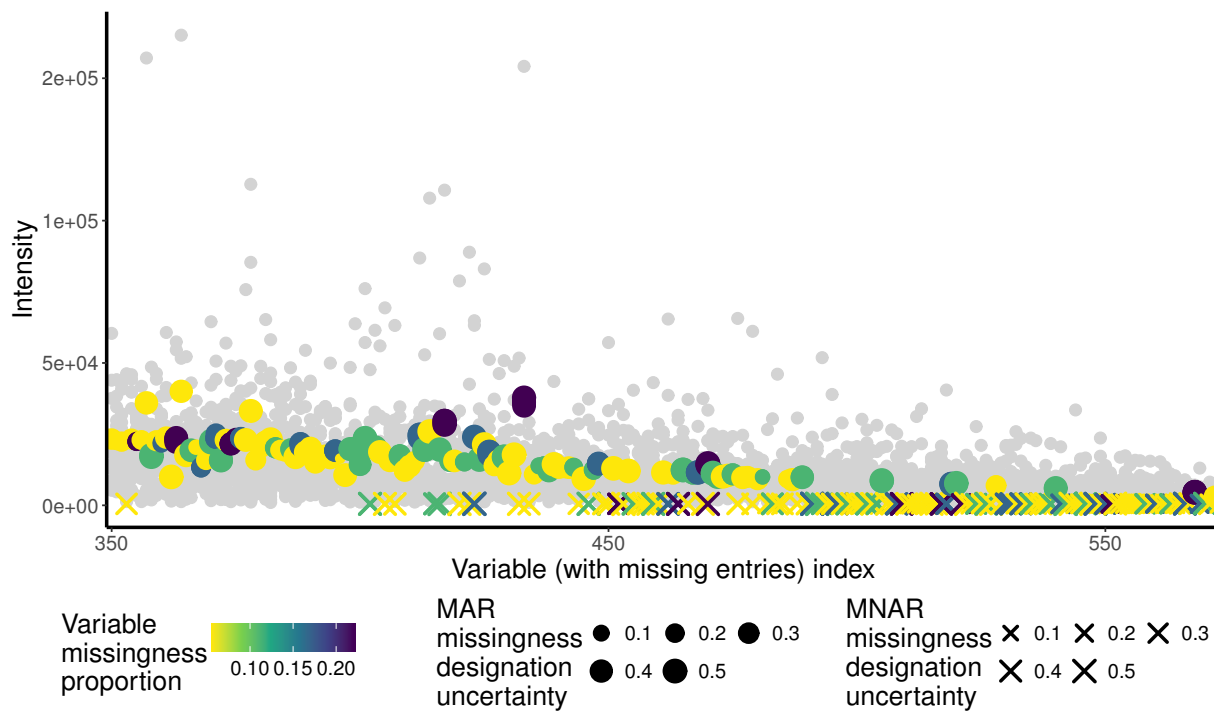
Addressing the issue of missing data in high-dimensional metabolomics data is important, as data acquisition can be difficult and expensive, and many commonly used analysis methods require a complete dataset. The proposed tIFA approach provides a statistically principled approach to imputing such missing data: it ensures that different types of missingness are accounted for, that the resulting imputed values have meaning for the user, and that the inherent uncertainty in both the imputed values and the missing data type is available. Further, tIFA provides a parsimonious model for metabolomics data that accounts for its typical $n \ll p$ dimensionality and high levels of dependence between variables. Comprehensive simulation studies demonstrate the performance of tIFA; physically meaningful imputed values are provided, and the advantages of tIFA are emphasised in comparison to existing imputation methods. Application of tIFA to a urinary LC-MS metabolomics dataset highlights its utility, which is facilitated through the provision of open-source R code.

The tIFA approach could be extended in several ways. The proposed model assumes data are distributed according to a truncated Gaussian distribution: different distributional assumptions could be used in order to increase flexibility and account for the typically heavier tailed metabolomics data. The use of truncated versions of the multivariate t (Lee et al., 2022) or multivariate normal inverse Gaussian (Barndorff-Nielsen, 1997) distributions, for example, within the tIFA framework are currently under investigation.

While a multiplicative truncated gamma process shrinkage prior was employed here to obviate the need to fit multiple models and use model selection criteria to choose the number of effective factors, there are several alternative shrinkage priors that may also be useful. For example, Indian buffet process priors (Knowles and Ghahramani, 2011) and spike-and-slab priors (Legramanti et al., 2020) are natural and straightforward alternatives. Further, the unordered generalised lower triangular representation of the loadings in a sparse Bayesian factor model provides posterior inference on the number of factors (Frühwirth-Schnatter



(a)



(b)

Figure 6: Observed and tIFA-imputed values for the 573 variables with missing values in the urinary metabolomics dataset. Observed values are shown in grey. All 573 variables with missing entries are shown in (a), while (b) shows a zoomed view of 224 later variables (with missingness) given their lower observed values and proximity to the LOD.

et al., 2024) and could be useful here.

More complicated missing data scenarios than that considered here often arise in metabolomics data. For example, there are challenges in longitudinal metabolomics data whereby missingness varies over time, or indeed entire timepoints in a study may be missing. Imputation in such complex missing data scenarios will require extensions to the imputation approach proposed here. The use of auto-regressive models for high-dimensional, longitudinal metabolomics data has been proposed (Nyamundanda et al., 2014); extending such models to handle missing data could be fruitful as could general approaches to longitudinal missing data imputation (Daniels and Hogan, 2008). In general, but particularly for these potential extensions, tIFA would benefit from increased computational efficiency. Alternative, more computationally efficient inferential approaches could be investigated, for example, through the use of variational or Hamiltonian Monte Carlo methods.

7 Acknowledgements

The authors would like to thank Dr Szymon Urbas for useful discussions which contributed to this work.

This publication has emanated from research conducted with the financial support of Science Foundation Ireland under Grant number 18/CRT/6049. For the purpose of Open Access, the author has applied a CC BY public copyright licence to any Author Accepted Manuscript version arising from this submission.

References

- Barndorff-Nielsen, O. E. (1997). Normal inverse Gaussian distributions and stochastic volatility modelling. *Scand. J. Stat.*, 24(1):1–13.
- Bartholomew, D., Knott, M., and Moustaki, I. (2011). *Latent variable models and factor analysis: a unified approach*. John Wiley & Sons, Ltd, Chichester, 3rd edition.

- Bhattacharya, A. and Dunson, D. B. (2011). Sparse Bayesian infinite factor models. *Biometrika*, 98(2):291–306.
- Bijlsma, S., Bobeldijk, I., Verheij, E. R., Ramaker, R., Kochhar, S., Macdonald, I. A., van Ommen, B., and Smilde, A. K. (2006). Large-scale human metabolomics studies: a strategy for data (pre-) processing and validation. *Anal. Chem.*, 78(2):567–574.
- Blaise, B. J., Correia, G., Tin, A., Young, J. H., Vergnaud, A.-C., Lewis, M., Pearce, J. T. M., Elliott, P., Nicholson, J. K., Holmes, E., and Ebbels, T. M. D. (2016). Power analysis and sample size determination in metabolic phenotyping. *Anal. Chem.*, 88(10):5179–5188.
- Box, G. E. and Tiao, G. C. (1973). *Bayesian inference in statistical analysis*. Addison-Wesley Publishing Company. Inc, Reading, 1st edition.
- D’Angelo, S., Brennan, L., and Gormley, I. C. (2021). Inferring food intake from multiple biomarkers using a latent variable model. *Ann. Appl. Stat.*, 15(4):2043–2060.
- Daniels, M. J. and Hogan, J. W. (2008). *Missing data in longitudinal studies: strategies for Bayesian modeling and sensitivity analysis*. Chapman and Hall/CRC, New York, 1st edition.
- Durante, D. (2017). A note on the multiplicative gamma process. *Stat. Probab. Lett.*, 122:198–204.
- Frühwirth-Schnatter, S. (2023). Generalized cumulative shrinkage process priors with applications to sparse Bayesian factor analysis. *Philos. Trans. R. Soc. A Math. Phys. Eng. Sci.*, 381(2247):20220148.
- Frühwirth-Schnatter, S., Hosszejni, D., and Lopes, H. F. (2024). Sparse Bayesian factor analysis when the number of factors is unknown. *Bayesian Anal.* Advance Publication.
- Gelfand, A. E., Smith, A. F. M., and Lee, T.-M. (1992). Bayesian analysis of constrained parameter and truncated data problems using Gibbs sampling. *J. Am. Stat. Assoc.*, 87(418):523–532.

- Gromski, P. S., Xu, Y., Kotze, H. L., Correa, E., Ellis, D. I., Armitage, E. G., Turner, M. L., and Goodacre, R. (2014). Influence of missing values substitutes on multivariate analysis of metabolomics data. *Metabolites*, 4(2):433–452.
- Gwee, X. Y., Gormley, I. C., and Fop, M. (2024). A latent shrinkage position model for binary and count network data. *Bayesian Anal.* In press.
- Hastie, T. and Mazumder, R. (2021). *softImpute: matrix completion via iterative soft-thresholded SVD*. R package version 1.4-1.
- Huang, J., Liu, J., Wang, K., Yang, Z., and Liu, X. (2018). Classification and identification of molecules through factor analysis method based on terahertz spectroscopy. *Spectrochim. Acta Part A Mol. Biomol. Spectrosc.*, 198:198–203.
- Knowles, D. and Ghahramani, Z. (2011). Nonparametric Bayesian sparse factor models with application to gene expression modeling. *Ann. Appl. Stat.*, 5(2B):1534–1552.
- Kosmidis, A. K., Kamisoglu, K., Calvano, S. E., Corbett, S. A., and Androulakis, I. P. (2013). Metabolomic fingerprinting: challenges and opportunities. *Crit. Rev. Biomed. Eng.*, 41(3):205–221.
- Lee, J., Jo, S., and Lee, J. (2022). Robust sparse Bayesian infinite factor models. *Comput. Stat.*, 37(5):2693–2715.
- Legramanti, S., Durante, D., and Dunson, D. B. (2020). Bayesian cumulative shrinkage for infinite factorizations. *Biometrika*, 107(3):745–752.
- LeVatte, M., Keshteli, A. H., Zarei, P., and Wishart, D. S. (2021). Applications of metabolomics to precision nutrition. *Lifestyle Genomics*, 15(1):1–9.
- Liland, K. H. (2011). Multivariate methods in metabolomics – from pre-processing to dimension reduction and statistical analysis. *TrAC Trends Anal. Chem.*, 30(6):827–841.
- Little, R. J. A. and Rubin, D. B. (2020). *Statistical analysis with missing data*. John Wiley & Sons, Inc, Hoboken, 3rd edition.

- McNamara, A. E., Yin, X., Collins, C., and Brennan, L. (2023). Metabolomic based approach to identify biomarkers of broccoli intake. *Food Funct.*, 14(18):8586–8596.
- McNicholas, P. D. and Murphy, T. B. (2008). Parsimonious Gaussian mixture models. *Stat. Comput.*, 18(3):285–296.
- Meng, C., Zeleznik, O. A., Thallinger, G. G., Kuster, B., Gholami, A. M., and Culhane, A. C. (2016). Dimension reduction techniques for the integrative analysis of multi-omics data. *Briefings Bioinforma.*, 17(4):628–641.
- Murphy, K., Viroli, C., and Gormley, I. C. (2020). Infinite mixtures of infinite factor analysers. *Bayesian Anal.*, 15(3):937–963.
- Nordin, E., Landberg, R., Hellström, P. M., and Brunius, C. (2024). Exploration of differential responses to FODMAPs and gluten in people with irritable bowel syndrome- a double-blind randomized cross-over challenge study. *Metabolomics*, 20(2):21.
- Nyamundanda, G., Gormley, I. C., and Brennan, L. (2014). A dynamic probabilistic principal components model for the analysis of longitudinal metabolomics data. *J. R. Stat. Soc. Ser. C Appl. Stat.*, 63(5):763–782.
- Oba, S., Sato, M.-a., Takemasa, I., Monden, M., Matsubara, K.-i., and Ishii, S. (2003). A Bayesian missing value estimation method for gene expression profile data. *Bioinformatics*, 19(16):2088–2096.
- Pang, Z., Lu, Y., Zhou, G., Hui, F., Xu, L., Viau, C., Spigelman, A. F., MacDonald, P. E., Wishart, D. S., Li, S., and Xia, J. (2024). MetaboAnalyst 6.0: towards a unified platform for metabolomics data processing, analysis and interpretation. *Nucleic Acids Res.*, 52(W1):W398–W406.
- R Core Team (2024). *R: a language and environment for statistical computing*. R Foundation for Statistical Computing, Vienna, Austria.
- Schiavon, L., Canale, A., and Dunson, D. B. (2022). Generalized infinite factorization models. *Biometrika*, 109(3):817–835.

- Shah, J., Brock, G. N., and Gaskins, J. (2019). BayesMetab: treatment of missing values in metabolomic studies using a Bayesian modeling approach. *BMC Bioinforma.*, 20(24):673.
- Shah, J. S., Rai, S. N., DeFilippis, A. P., Hill, B. G., Bhatnagar, A., and Brock, G. N. (2017). Distribution based nearest neighbor imputation for truncated high dimensional data with applications to pre-clinical and clinical metabolomics studies. *BMC Bioinforma.*, 18(1):114.
- Spicer, R., Salek, R. M., Moreno, P., Cañueto, D., and Steinbeck, C. (2017). Navigating freely-available software tools for metabolomics analysis. *Metabolomics*, 13(9):106.
- Stekhoven, D. J. (2022). *missForest: nonparametric missing value imputation using random forest*. R package version 1.5.
- Stekhoven, D. J. and Bühlmann, P. (2012). MissForest—non-parametric missing value imputation for mixed-type data. *Bioinformatics*, 28(1):112–118.
- Sun, J. and Xia, Y. (2024). Pretreating and normalizing metabolomics data for statistical analysis. *Genes Dis.*, 11(3):100979.
- Taylor, S., Ponzini, M., Wilson, M., and Kim, K. (2021). Comparison of imputation and imputation-free methods for statistical analysis of mass spectrometry data with missing data. *Briefings Bioinforma.*, 23(1):bbab353.
- Tounta, V., Liu, Y., Cheyne, A., and Larrouy-Maumus, G. (2021). Metabolomics in infectious diseases and drug discovery. *Mol. Omi.*, 17(3):376–393.
- Wei, R., Wang, J., Jia, E., Chen, T., Ni, Y., and Jia, W. (2018a). GSimp: a Gibbs sampler based left-censored missing value imputation approach for metabolomics studies. *PLOS Comput. Biol.*, 14(1):e1005973.
- Wei, R., Wang, J., Su, M., Jia, E., Chen, S., Chen, T., and Ni, Y. (2018b). Missing value imputation approach for mass spectrometry-based metabolomics data. *Sci. Reports*, 8(1):663.

- Wilson, M. D., Ponzini, M. D., Taylor, S. L., and Kim, K. (2022). Imputation of missing values for multi-biospecimen metabolomics studies: bias and effects on statistical validity. *Metabolites*, 12(7):671.
- Wishart, D. S., Guo, A., Oler, E., Wang, F., Anjum, A., Peters, H., Dizon, R., Sayeeda, Z., Tian, S., Lee, B. L., Berjanskii, M., Mah, R., Yamamoto, M., Jovel, J., Torres-Calzada, C., Hiebert-Giesbrecht, M., Lui, V. W., Varshavi, D., Varshavi, D., Allen, D., Arndt, D., Khetarpal, N., Sivakumaran, A., Harford, K., Sanford, S., Yee, K., Cao, X., Budinski, Z., Liigand, J., Zhang, L., Zheng, J., Mandal, R., Karu, N., Dambrova, M., Schiöth, H. B., Greiner, R., and Gautam, V. (2022). HMDB 5.0: the human metabolome database for 2022. *Nucleic Acids Res.*, 50(D1):D622–D631.
- Wörheide, M. A., Krumsiek, J., Kastenmüller, G., and Arnold, M. (2021). Multi-omics integration in biomedical research – a metabolomics-centric review. *Anal. Chim. Acta*, 1141:144–162.
- Worley, B. and Powers, R. (2013). Multivariate analysis in metabolomics. *Curr. Metabolomics*, 1(1):92–107.
- Zhao, X., Niu, L., Clerici, C., Russo, R., Byrd, M., and Setchell, K. D. R. (2019). Data analysis of MS-based clinical lipidomics studies with crossover design: a tutorial mini-review of statistical methods. *Clin. Mass Spectrom.*, 13:5–17.
- Zhong, P., Wei, X., Li, X., Wei, X., Wu, S., Huang, W., Koidis, A., Xu, Z., and Lei, H. (2022). Untargeted metabolomics by liquid chromatography-mass spectrometry for food authentication: a review. *Compr. Rev. Food Sci. Food Saf.*, 21(3):2455–2488.

A Full conditional posterior distributions

Full conditional posterior distributions for each parameter of the tIFA model are available in closed form as detailed below. Derivations are provided in B. Note that in all cases, $\text{Ga}(\alpha, \beta)$ refers to the gamma distribution whose mean is given by $\frac{\alpha}{\beta}$. The notation $p(\theta | \dots)$ refers

to the conditional posterior distribution of θ given all other model parameters. Here, k^* is used as a finite approximation of the number of latent factors.

$$p(\boldsymbol{\lambda}_j \mid \dots) \sim N_{k^*}^{[0, \infty)}(\mathbf{A}, \mathbf{B})$$

where

$$\mathbf{B} = [\mathbf{D}_j^{-1} + \sigma_j^{-2} \sum_{i=1}^n \boldsymbol{\eta}_i \boldsymbol{\eta}_i^\top]^{-1}$$

$$\mathbf{A} = \mathbf{B} [\sigma_j^{-2} \sum_{i=1}^n (y_{ij} - \mu_j) \boldsymbol{\eta}_i]$$

and with $\mathbf{D}_j^{-1} = \text{diag}(\phi_{j1}\tau_1, \dots, \phi_{jk^*}\tau_{k^*})$.

$$p(\boldsymbol{\mu} \mid \dots) \sim N_p^{[0, \infty)}([n\boldsymbol{\Sigma}^{-1} + \varphi\mathbf{I}_p]^{-1}[\boldsymbol{\Sigma}^{-1} \sum_{i=1}^n (\mathbf{y}_i - \boldsymbol{\Lambda}\boldsymbol{\eta}_i) + \varphi\mathbf{I}_p\tilde{\boldsymbol{\mu}}], [n\boldsymbol{\Sigma}^{-1} + \varphi\mathbf{I}_p]^{-1})$$

$$p(\sigma_j^{-2} \mid \dots) \sim \text{Ga}(\frac{n}{2} + a_\sigma, b_\sigma + \frac{1}{2} \sum_{i=1}^n (y_{ij} - \mu_j - \boldsymbol{\lambda}_j^\top \boldsymbol{\eta}_i)^2)$$

$$p(\boldsymbol{\eta}_i \mid \dots) \sim N_{k^*}^{[0, \infty)}([\boldsymbol{\Lambda}^\top \boldsymbol{\Sigma}^{-1} \boldsymbol{\Lambda} + \mathbf{I}_{k^*}]^{-1} \boldsymbol{\Lambda}^\top \boldsymbol{\Sigma}^{-1} (\mathbf{y}_i - \boldsymbol{\mu}), [\boldsymbol{\Lambda}^\top \boldsymbol{\Sigma}^{-1} \boldsymbol{\Lambda} + \mathbf{I}_{k^*}]^{-1})$$

$$p(\phi_{jh} \mid \dots) \sim \text{Ga}(\frac{1}{2} + \kappa_1, \frac{\tau_h \lambda_{jh}^2}{2} + \kappa_2)$$

$$p(\delta_1 \mid \dots) \sim \text{Ga}(a_1 + \frac{pk^*}{2}, 1 + \frac{\sum_{l=1}^{k^*} \tau_l^{(1)} \sum_{j=1}^p \phi_{jl} \lambda_{jl}^2}{2})$$

$$p(\delta_h \mid \dots) \sim \text{Ga}^{[1, \infty)}(a_2 + \frac{p(k^* - h + 1)}{2}, 1 + \frac{\sum_{l=h}^{k^*} \tau_l^{(h)} \sum_{j=1}^p \phi_{jl} \lambda_{jl}^2}{2}), \quad h \geq 2$$

where $\tau_l^{(h)} = \prod_{t=1, t \neq h}^l \delta_t$ for $h = 1, \dots, k^*$.

$$p(\alpha \mid \dots) \propto \text{Beta}(N_m^{LOD^+} + 1, N_o^{LOD^+} + 1)$$

where $N_m^{LOD^+}$ is the number of points inferred to be missing above the LOD and $N_o^{LOD^+}$ is the number of points observed above the LOD.

B Derivation of full conditional posterior distributions

In order to derive the full conditional posterior distributions for the tIFA model, one can first complete the derivations for the unconstrained case and then simply apply the relevant truncation to the unconstrained posterior (Box and Tiao, 1973; Gelfand et al., 1992). This approach is utilised in the case of the conditional posterior distributions of parameters Λ , η , and μ . The full conditional posterior distributions for Σ , ϕ , δ , and α are straightforward to derive, as their prior distributions are naturally constrained by their respective supports. Thus the derivation of their respective conditional posterior distributions is unchanged from the unconstrained case.

The model likelihood and prior distributions are as detailed in Sections 3.1 and 3.3, giving the posterior distribution as

$$p(\mu, \Lambda, \eta, \Sigma, \phi, \delta, \alpha \mid \mathbf{Y}) \propto p(\mathbf{Y} \mid \mu, \eta, \Lambda, \Sigma) p(\mu) p(\eta) p(\Sigma) p(\Lambda \mid \phi, \tau) \\ p(\phi) p(\delta) p(\alpha).$$

From this, full conditional distributions can be derived. Note that k is used throughout to denote the assumed infinite number of latent factors, however, in practice some finite k^* is used for computational reasons.

B.1 Deriving the full conditional posterior distribution for the mean

$$p(\mu \mid \dots) \propto \prod_{i=1}^n [p(\mathbf{y}_i \mid \dots)] p(\mu)$$

$$p(\boldsymbol{\mu} \mid \dots) \propto \prod_{i=1}^n [N_p(\boldsymbol{\mu} + \boldsymbol{\Lambda}\boldsymbol{\eta}_i, \boldsymbol{\Sigma})] N_p(\tilde{\boldsymbol{\mu}}, \varphi^{-1}\mathbf{I}_p)$$

$$p(\boldsymbol{\mu} \mid \dots) \propto \exp \left\{ -\frac{1}{2} [\boldsymbol{\mu}^\top (n\boldsymbol{\Sigma}^{-1} + \varphi\mathbf{I}_p) \boldsymbol{\mu} - 2\boldsymbol{\mu}^\top (\boldsymbol{\Sigma}^{-1} \sum_{i=1}^n (\mathbf{y}_i - \boldsymbol{\Lambda}\boldsymbol{\eta}_i) + \varphi\mathbf{I}_p\tilde{\boldsymbol{\mu}})] \right\}$$

Thus

$$p(\boldsymbol{\mu} \mid \dots) \sim N_p([n\boldsymbol{\Sigma}^{-1} + \varphi\mathbf{I}_p])^{-1} [\boldsymbol{\Sigma}^{-1} \sum_{i=1}^n (\mathbf{y}_i - \boldsymbol{\Lambda}\boldsymbol{\eta}_i) + \varphi\mathbf{I}_p\tilde{\boldsymbol{\mu}}, [n\boldsymbol{\Sigma}^{-1} + \varphi\mathbf{I}_p]^{-1}).$$

B.2 Deriving the full conditional posterior distribution for a row of the loadings matrix

For each row of the loadings matrix $j = 1, \dots, p$:

$$p(\boldsymbol{\lambda}_j \mid \dots) \propto \prod_{i=1}^n [p(y_{ij} \mid \dots)] p(\boldsymbol{\lambda}_j \mid \phi_j, \tau)$$

$$p(\boldsymbol{\lambda}_j \mid \dots) \propto \prod_{i=1}^n [N_1(\mu_j + \boldsymbol{\lambda}_j^\top \boldsymbol{\eta}_i, \sigma_j^{-2})] N_k(\mathbf{0}, \mathbf{D}_j)$$

where $\mathbf{D}_j^{-1} = \text{diag}(\phi_{j1}\tau_1, \dots, \phi_{jk}\tau_k)$.

$$p(\boldsymbol{\lambda}_j \mid \dots) \propto \exp \left\{ -\frac{1}{2} [\boldsymbol{\lambda}_j^\top (\mathbf{D}_j^{-1} + \sigma_j^{-2} \sum_{i=1}^n \boldsymbol{\eta}_i \boldsymbol{\eta}_i^\top) \boldsymbol{\lambda}_j - 2\boldsymbol{\lambda}_j^\top (\sigma_j^{-2} \sum_{i=1}^n (y_{ij} - \mu_j) \boldsymbol{\eta}_i)] \right\}$$

Thus

$$p(\boldsymbol{\lambda}_j \mid \dots) \sim N_k(\mathbf{A}, \mathbf{B})$$

where

$$\mathbf{B} = [\mathbf{D}_j^{-1} + \sigma_j^{-2} \sum_{i=1}^n \boldsymbol{\eta}_i \boldsymbol{\eta}_i^\top]^{-1}$$

$$\mathbf{A} = \mathbf{B} \left[\sigma_j^{-2} \sum_{i=1}^n (y_{ij} - \mu_j) \boldsymbol{\eta}_i \right].$$

B.3 Deriving the full conditional posterior distribution for the diagonal entries of the specific errors' covariance matrix

For $j = 1, \dots, p$, for entry σ_j of the diagonal of the covariance matrix $\boldsymbol{\Sigma}$:

$$p(\sigma_j^{-2} | \dots) \propto \prod_{i=1}^n [p(y_{ij} | \dots)] p(\sigma_j^{-2})$$

$$p(\sigma_j^{-2} | \dots) \propto \prod_{i=1}^n [N_1(\mu_j + \boldsymbol{\lambda}_j^\top \boldsymbol{\eta}_i, \sigma_j^2)] \text{Ga}(a_\sigma, b_\sigma)$$

$$p(\sigma_j^{-2} | \dots) \propto (\sigma_j^{-2})^{\frac{n}{2} + a_\sigma - 1} \exp \left\{ -\sigma_j^{-2} \left[b_\sigma + \frac{1}{2} \sum_{i=1}^n (y_{ij} - \mu_j - \boldsymbol{\lambda}_j^\top \boldsymbol{\eta}_i)^2 \right] \right\}$$

Thus

$$p(\sigma_j^{-2} | \dots) \sim \text{Ga} \left(\frac{n}{2} + a_\sigma, b_\sigma + \frac{1}{2} \sum_{i=1}^n (y_{ij} - \mu_j - \boldsymbol{\lambda}_j^\top \boldsymbol{\eta}_i)^2 \right).$$

B.4 Deriving the full conditional posterior distributions for the latent factors

For each $i = 1, \dots, n$:

$$p(\boldsymbol{\eta}_i | \dots) \propto p(\mathbf{y}_i | \dots) p(\boldsymbol{\eta}_i)$$

$$p(\boldsymbol{\eta}_i | \dots) \propto N_p(\boldsymbol{\mu} + \boldsymbol{\Lambda} \boldsymbol{\eta}_i, \boldsymbol{\Sigma}) N_k(\mathbf{0}, \mathbf{I}_k)$$

$$p(\boldsymbol{\eta}_i | \dots) \propto \exp \left\{ -\frac{1}{2} \left[\boldsymbol{\eta}_i^\top (\boldsymbol{\Lambda}^\top \boldsymbol{\Sigma}^{-1} \boldsymbol{\Lambda} + \mathbf{I}_k) \boldsymbol{\eta}_i - 2 \boldsymbol{\eta}_i^\top (\boldsymbol{\Lambda}^\top \boldsymbol{\Sigma}^{-1} (\mathbf{y}_i - \boldsymbol{\mu})) \right] \right\}$$

Thus

$$p(\boldsymbol{\eta}_i | \dots) \propto N_k \left(\left[\boldsymbol{\Lambda}^\top \boldsymbol{\Sigma}^{-1} \boldsymbol{\Lambda} + \mathbf{I}_k \right]^{-1} \boldsymbol{\Lambda}^\top \boldsymbol{\Sigma}^{-1} (\mathbf{y}_i - \boldsymbol{\mu}), \left[\boldsymbol{\Lambda}^\top \boldsymbol{\Sigma}^{-1} \boldsymbol{\Lambda} + \mathbf{I}_k \right]^{-1} \right).$$

B.5 Deriving the full conditional posterior distributions for the local shrinkage parameters

For $j = 1, \dots, p$ and $h = 1, \dots, k$:

$$p(\phi_{jh} \mid \dots) \propto p(\lambda_{jh} \mid \phi_{jh}, \tau_h) p(\phi_{jh})$$

$$p(\phi_{jh} \mid \dots) \propto N_1(0, \phi_{jh}^{-1} \tau_h^{-1}) \text{Ga}(\kappa_1, \kappa_2)$$

$$p(\phi_{jh} \mid \dots) \propto (\phi_{jh})^{\frac{1}{2} + \kappa_1 - 1} \exp \left\{ -\phi_{jh} \left[\frac{\lambda_{jh}^2 \tau_h}{2} + \kappa_2 \right] \right\}$$

Thus

$$p(\phi_{jh} \mid \dots) \sim \text{Ga}\left(\frac{1}{2} + \kappa_1, \frac{\lambda_{jh}^2 \tau_h}{2} + \kappa_2\right).$$

B.6 Deriving the full conditional posterior distributions for the multiplicative shrinkage parameters

Separate derivations are provided for δ_h for $h = 1$ and for $h = 2, \dots, k$. Beginning with δ_1 :

$$p(\delta_1 \mid \dots) \propto \prod_{l=1}^k \prod_{j=1}^p [p(\lambda_{jl} \mid \phi_{jl}, \tau_l)] p(\delta_1)$$

$$p(\delta_1 \mid \dots) \propto \prod_{l=1}^k \prod_{j=1}^p [N_1(0, \phi_{jl}^{-1} \tau_l^{-1})] \text{Ga}(a_1, 1)$$

$$p(\delta_1 \mid \dots) \propto \delta_1^{\frac{pk}{2} + a_1 - 1} \exp \left\{ -\delta_1 \left[1 + \frac{1}{2} \sum_{l=1}^k \tau_l^{(1)} \sum_{j=1}^p \lambda_{jl}^2 \phi_{jl} \right] \right\}$$

Thus

$$p(\delta_1 \mid \dots) \propto \text{Ga}\left(\frac{pk}{2} + a_1, 1 + \frac{1}{2} \sum_{l=1}^k \tau_l^{(1)} \sum_{j=1}^p \lambda_{jl}^2 \phi_{jl}\right).$$

Similarly for the remaining δ_h parameters, for $h \geq 2$

$$p(\delta_h | \dots) \propto \text{Ga}^{[1, \infty)}\left(\frac{p(k-h+1)}{2} + a_2, 1 + \frac{1}{2} \sum_{l=h}^k \tau_l^{(h)} \sum_{j=1}^p \lambda_{jl}^2 \phi_{jl}\right), \quad h \geq 2$$

where $\tau_l^{(h)} = \prod_{t=1, t \neq h}^l \delta_t$ for $h = 1, \dots, k$.

B.7 Deriving the full conditional posterior distribution for the MAR missingness probability

The α parameter represents the probability that a data point is missing given that its true value is above the LOD. Given the assumptions of the missingness type, this amounts to the probability of a data entry being MAR, as all points with values less than the LOD are assumed MNAR. For points where MAR holds, one has that

$$p(y_{ij}, R_{ij} = 0 | \dots) = p(y_{ij}) p(R_{ij} = 0 | \dots)$$

$$p(y_{ij}, R_{ij} = 1 | \dots) = p(y_{ij}) p(R_{ij} = 1 | \dots).$$

Given the uninformative uniform prior on α , the full conditional posterior for α can therefore be derived as

$$p(\alpha | \dots) \propto \prod_{i=1}^n \prod_{j=1}^p p(R_{ij} = 0 | \dots) p(R_{ij} = 1 | \dots)$$

$$p(\alpha | \dots) \propto \alpha^{N_m^{LOD^+}} (1)^{N_m^{LOD^-}} (1 - \alpha)^{N_o^{LOD^+}} (1 - 1)^{N_o^{LOD^-}}$$

where $N_m^{LOD^+}$ is the number of points inferred to be missing above the LOD, $N_m^{LOD^-}$ is the number of points inferred to be missing below the LOD, $N_o^{LOD^+}$ is the number of points observed above the LOD, and $N_o^{LOD^-}$ is the number of points observed below the LOD (naturally 0). Hence

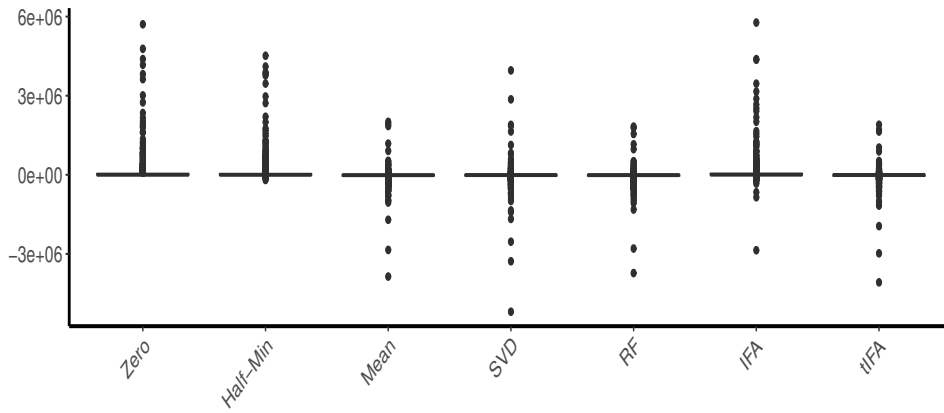
$$p(\alpha | \dots) \propto \alpha^{N_m^{LOD^+}} (1 - \alpha)^{N_o^{LOD^+}}$$

Thus

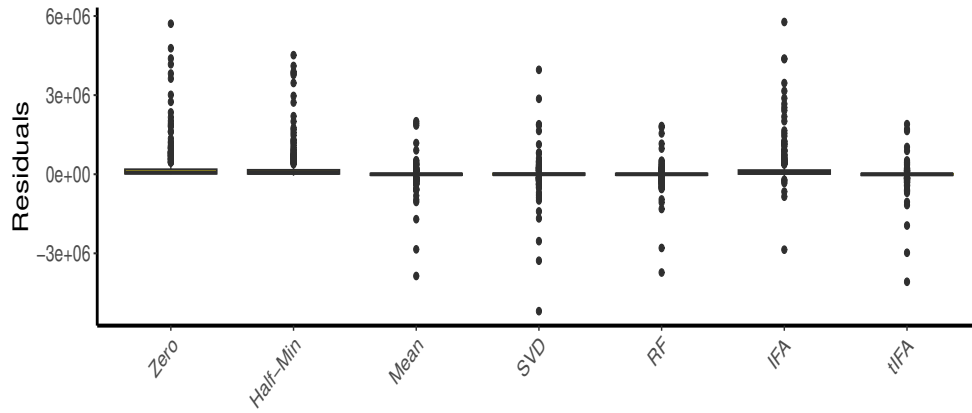
$$p(\alpha \mid \dots) \propto \text{Beta}(N_m^{LOD^+} + 1, N_o^{LOD^+} + 1).$$

C Additional simulation study materials

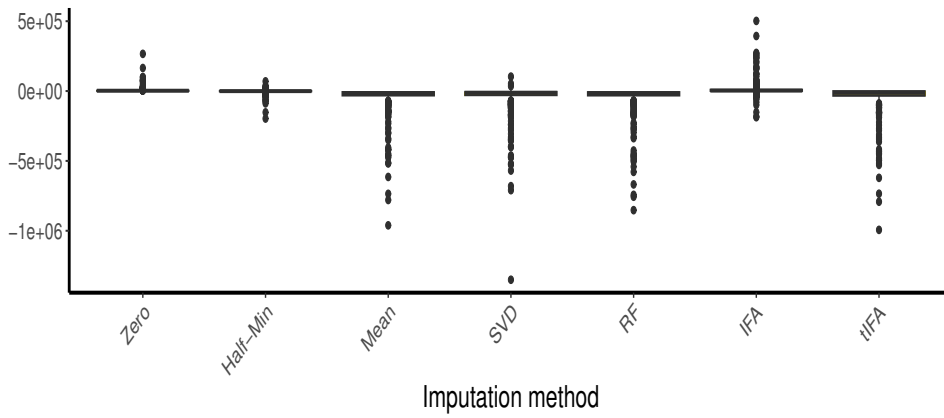
Further details of the simulation study presented in Section 4 are provided here. Figure C1 illustrates the residuals between posterior mean imputed values and true values under the imputation methods considered across all simulation replicates. For a single simulated dataset, Figures C2-C8 illustrate individual model residuals for zero, half-minimum, mean, SVD, RF, IFA, and tIFA imputation respectively, while Figures C9-C15 detail the difference between the true and imputed values.



(a)



(b)



(c)

Figure C1: Residuals between posterior mean imputed values and true values for (a) all imputed values, (b) MAR imputed values and (c) MNAR imputed values across ten simulated datasets, for all imputation methods considered.

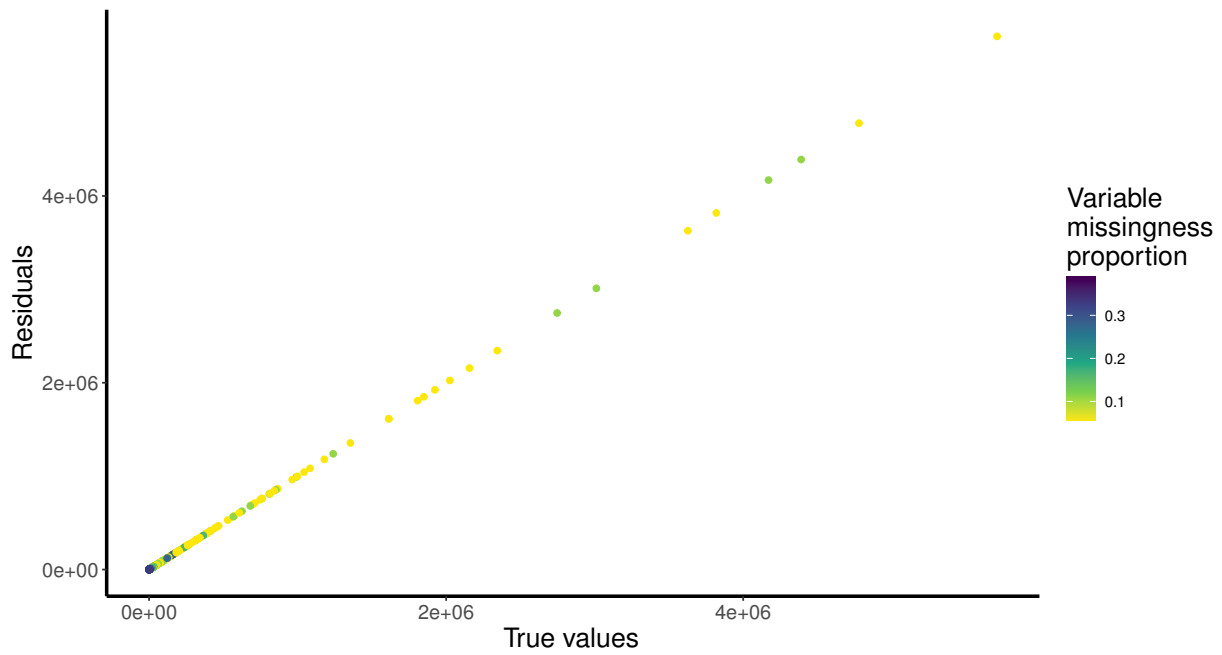


Figure C2: Residuals between posterior mean imputed values and true values under zero imputation for one simulated dataset.

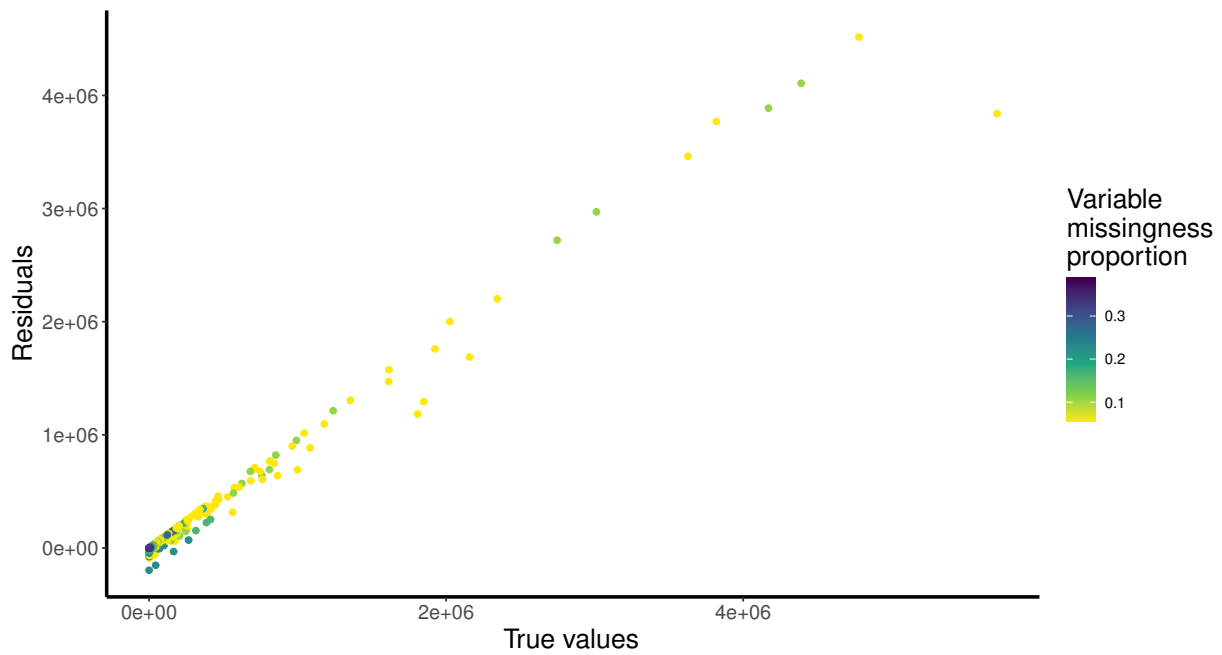


Figure C3: Residuals between posterior mean imputed values and true values under half-minimum imputation for one simulated dataset.

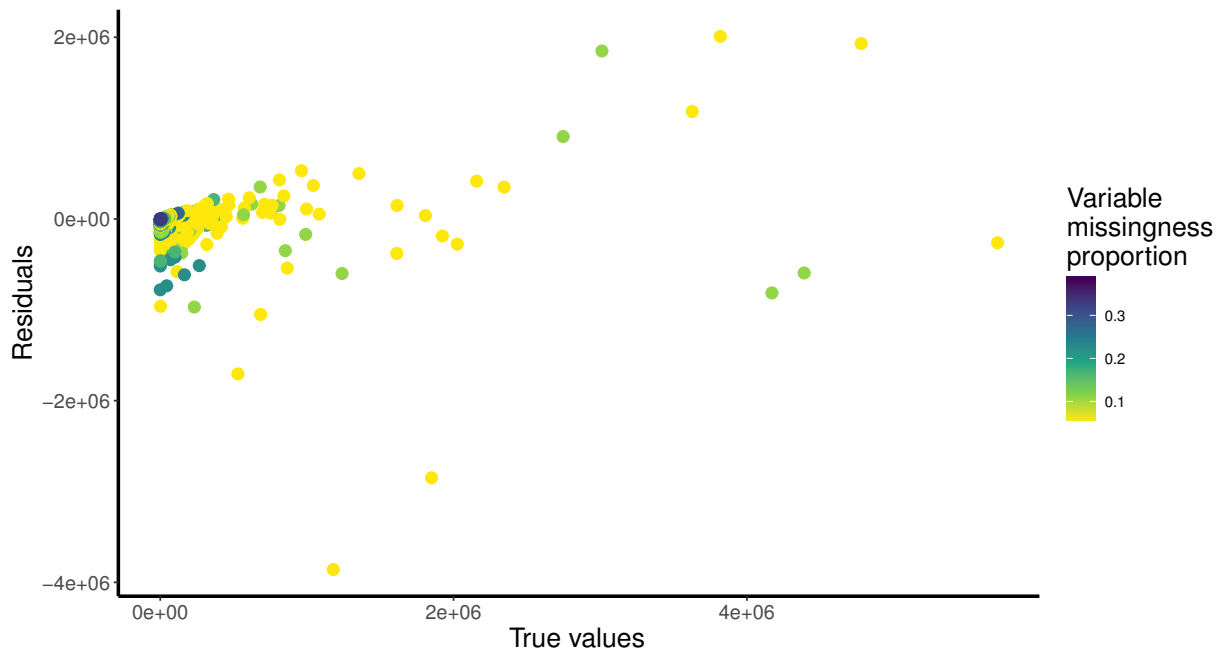


Figure C4: Residuals between posterior mean imputed values and true values under mean imputation for one simulated dataset.

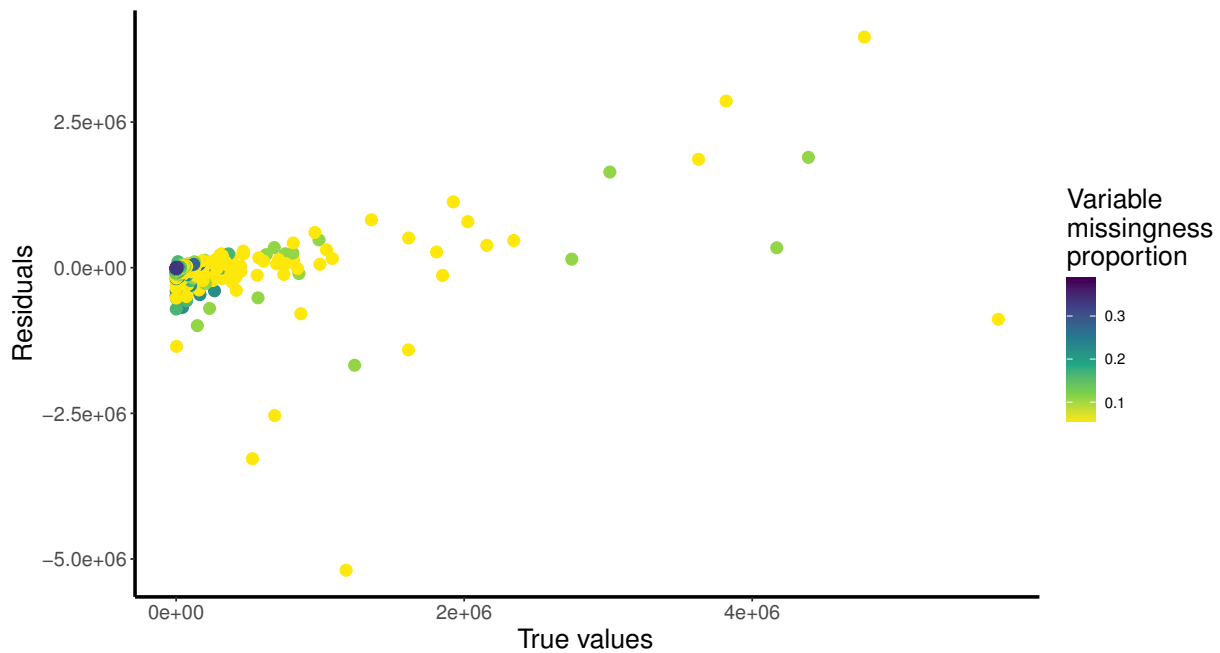


Figure C5: Residuals between posterior mean imputed values and true values under the SVD approach for one simulated dataset.

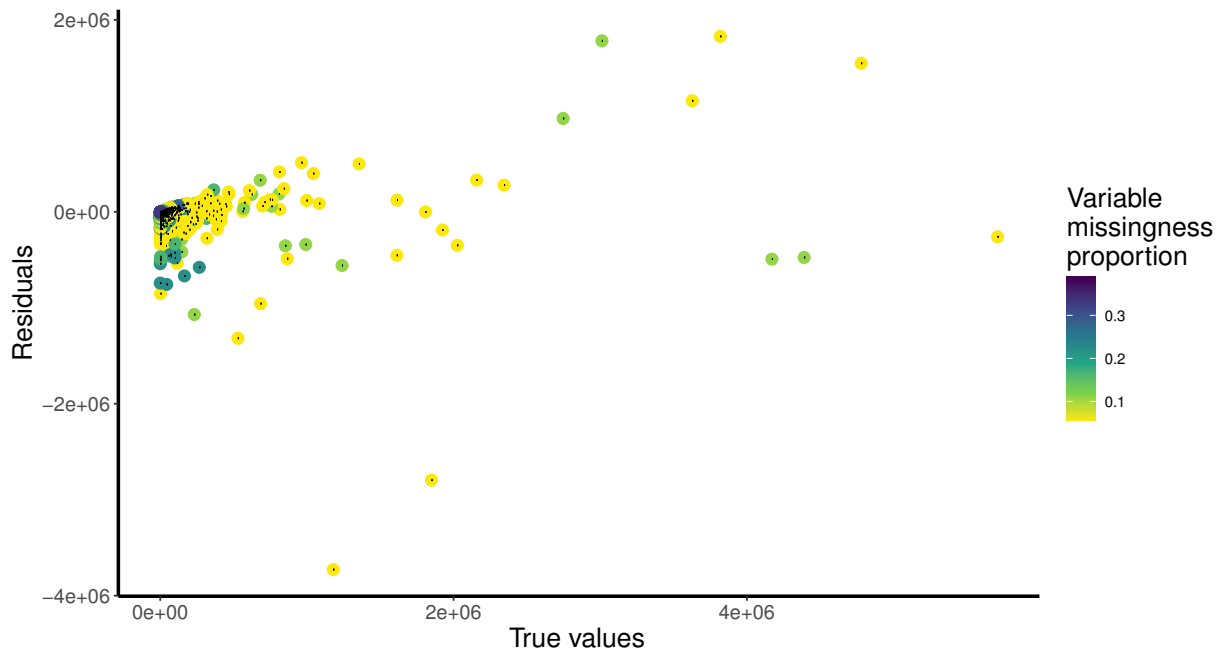


Figure C6: Residuals between posterior mean imputed values and true values under the RF approach for one simulated dataset.

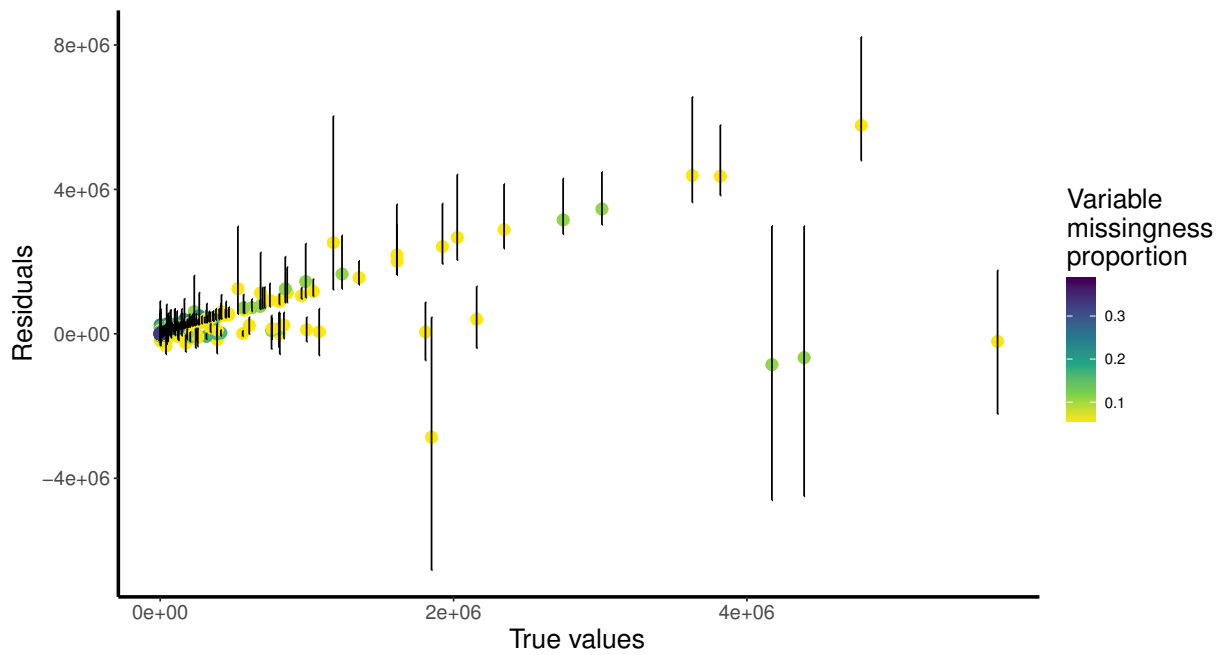


Figure C7: Residuals between posterior mean imputed values and true values under the IFA model for one simulated dataset.

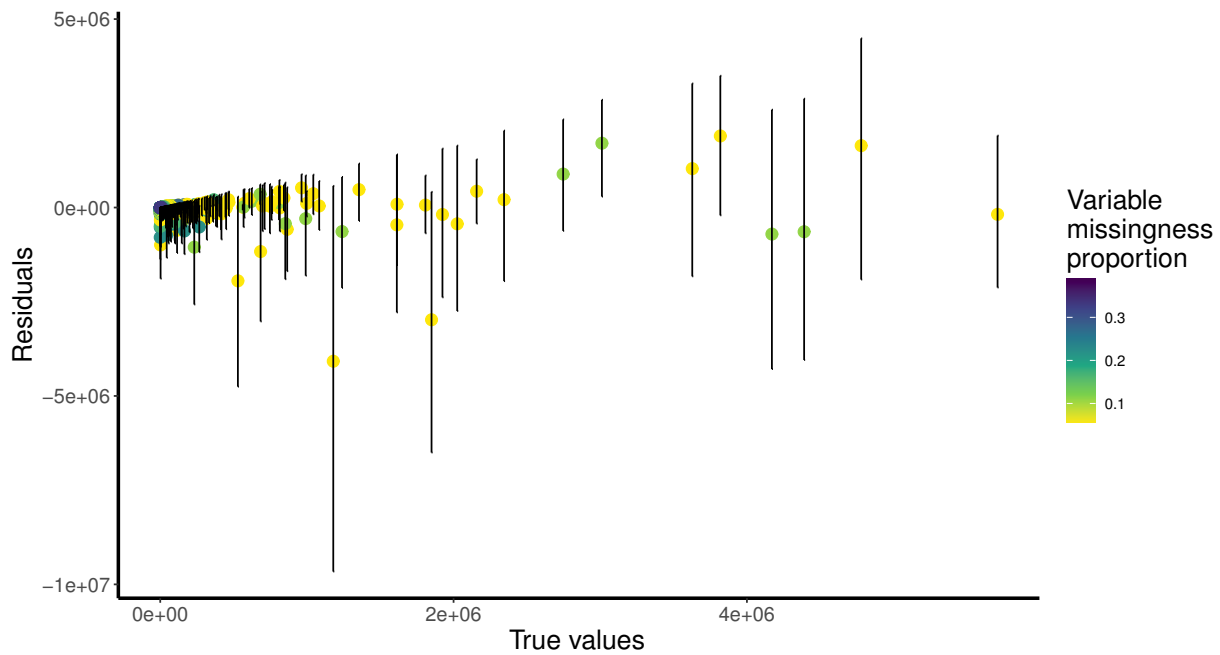


Figure C8: Residuals between posterior mean imputed values and true values under the tIFA model for one simulated dataset.

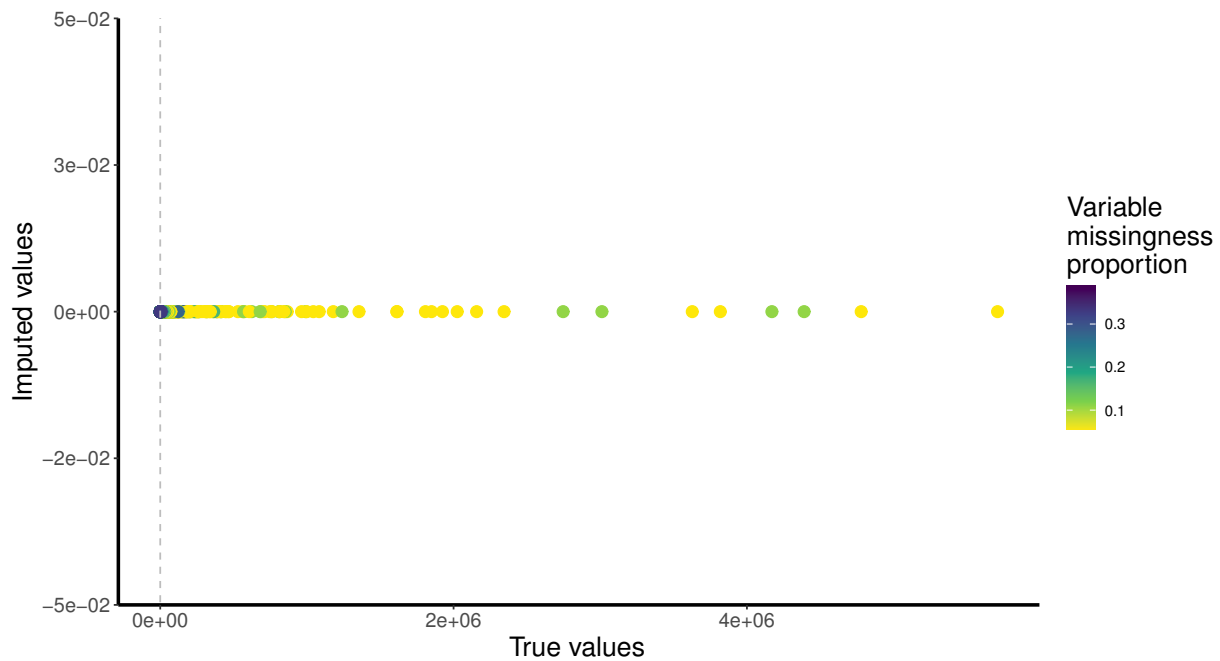


Figure C9: True versus imputed values under zero imputation for one simulated dataset. The dashed grey line is the line of equality.

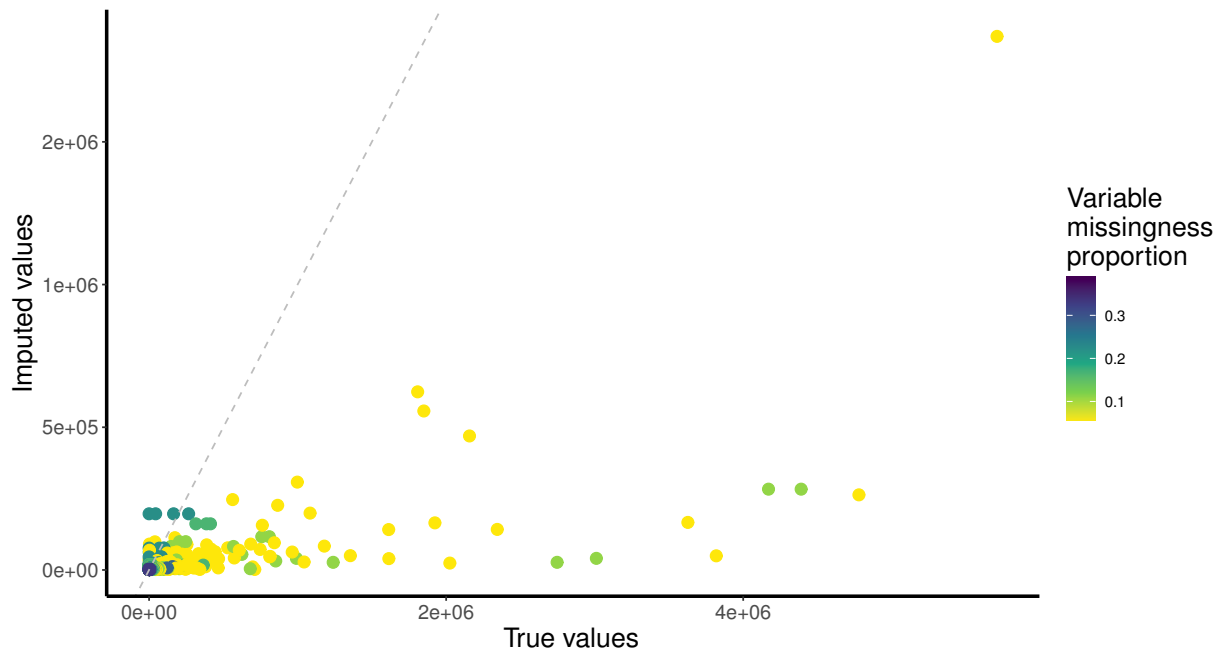


Figure C10: True versus imputed values under half-minimum imputation for one simulated dataset. The dashed grey line is the line of equality.

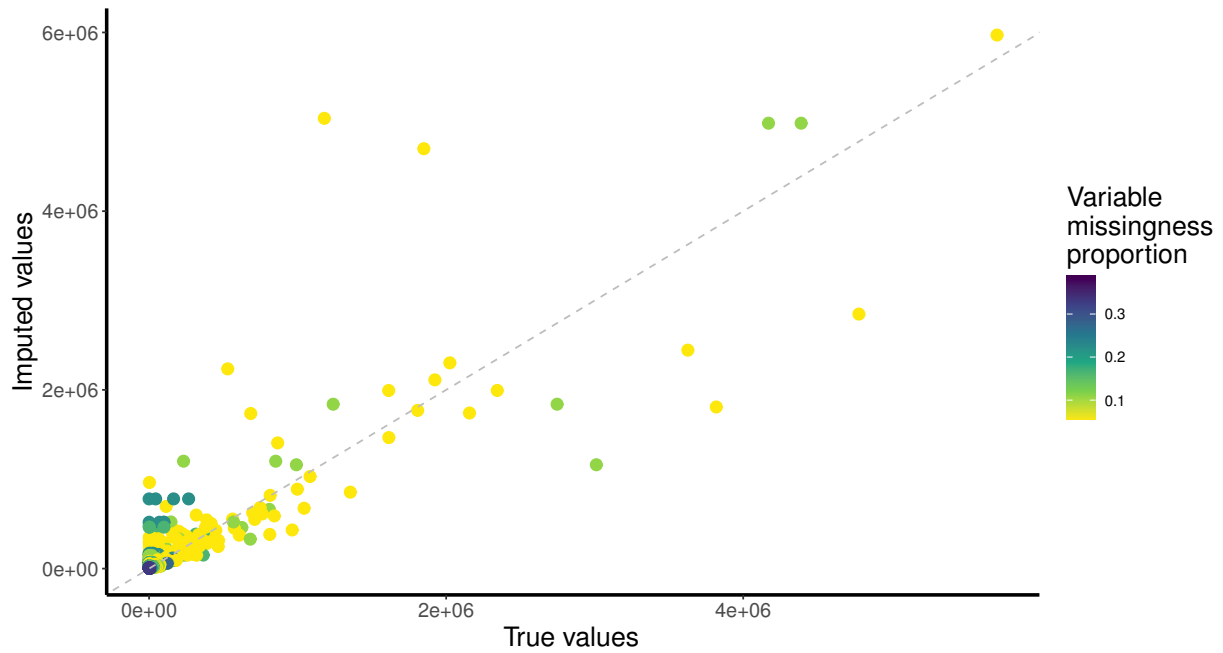


Figure C11: True versus imputed values under mean imputation for one simulated dataset. The dashed grey line is the line of equality.

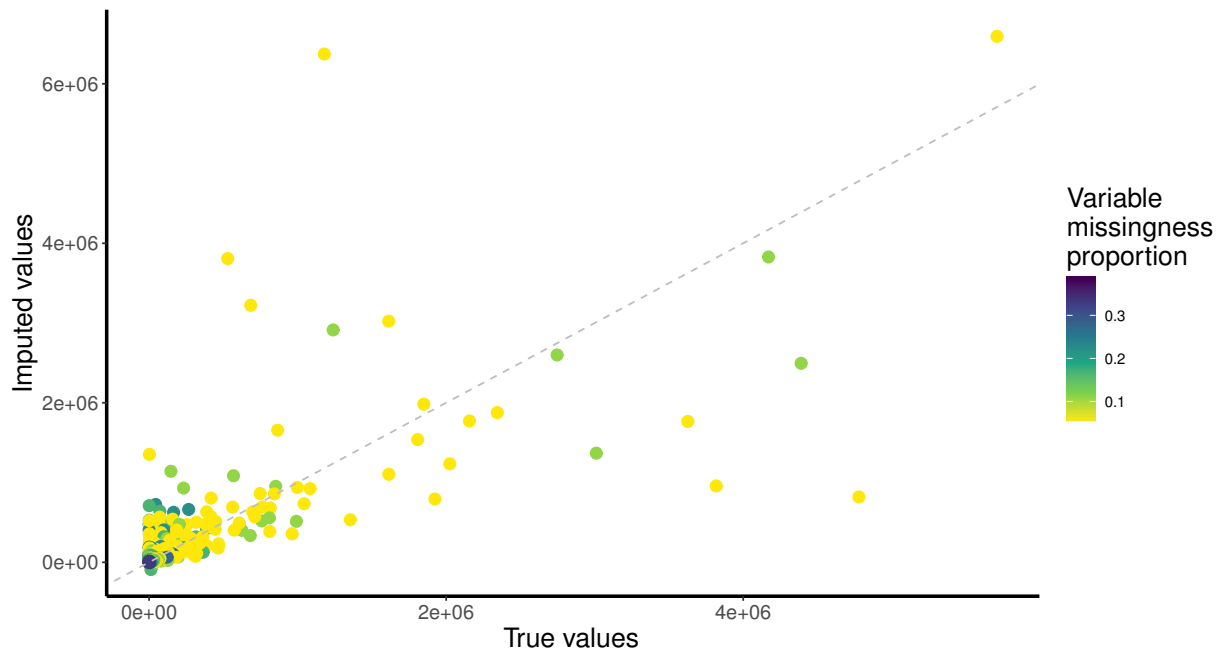


Figure C12: True versus imputed values under the SVD approach for one simulated dataset. The dashed grey line is the line of equality.

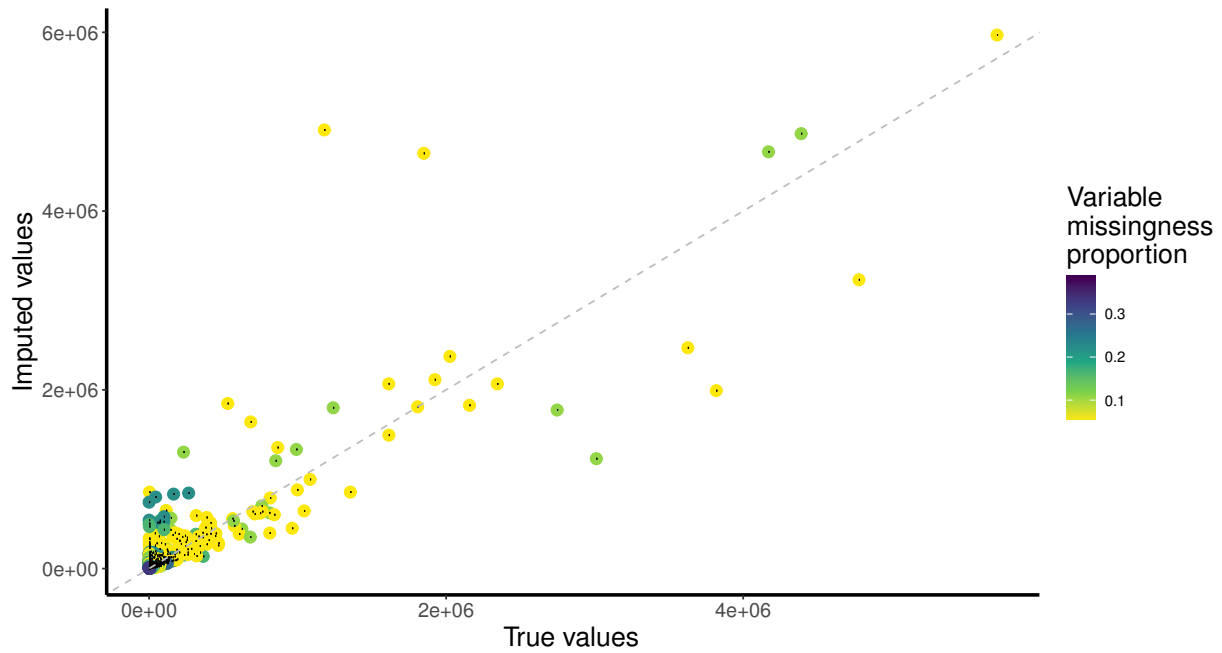


Figure C13: True versus imputed values under the RF approach for one simulated dataset. The dashed grey line is the line of equality.

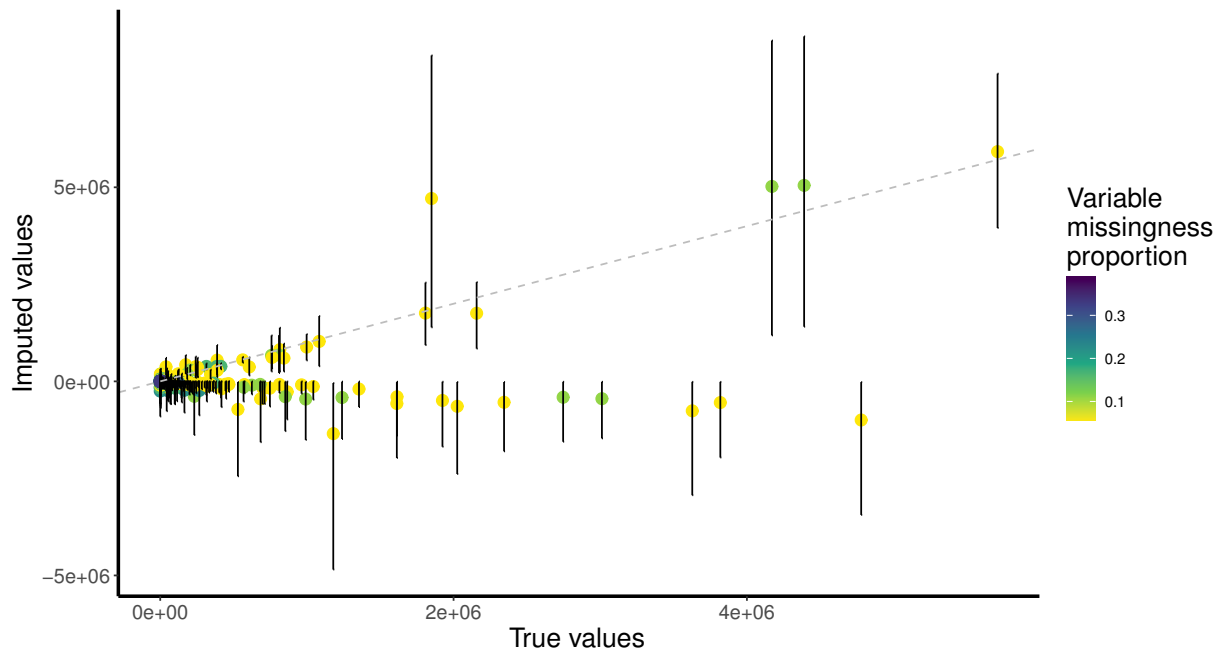


Figure C14: True versus imputed values under the IFA model for one simulated dataset. The dashed grey line is the line of equality.

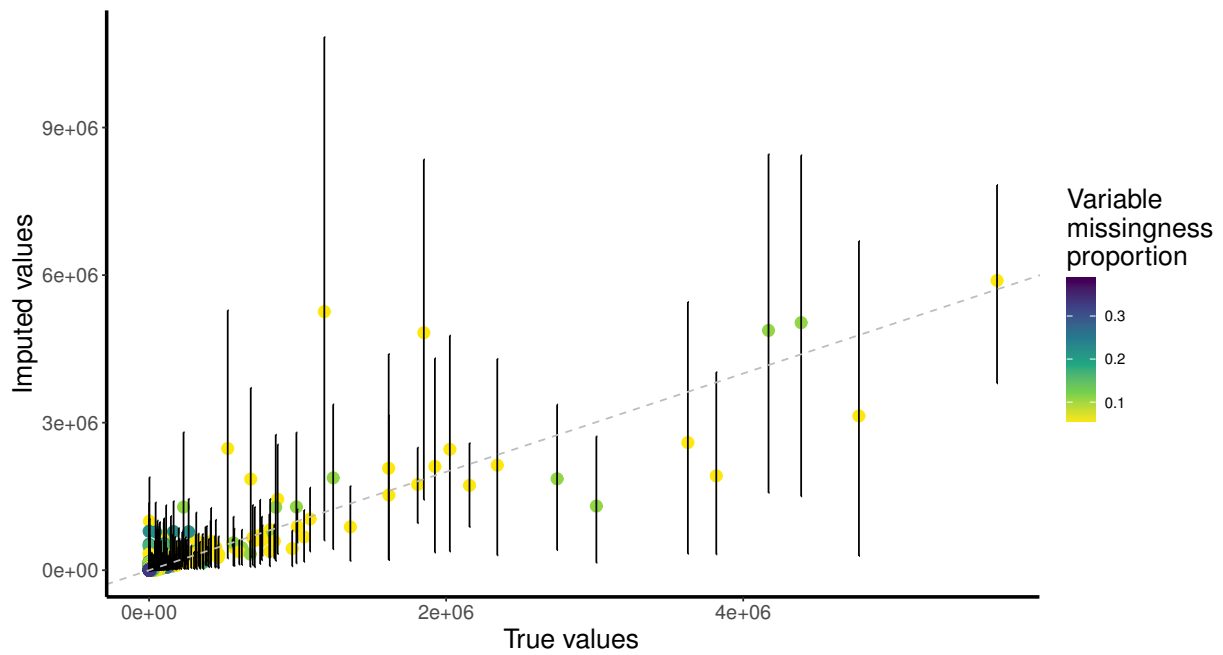


Figure C15: True versus imputed values under the tIFA model for one simulated dataset. The dashed grey line is the line of equality.